Materials physics on the atomistic scale

Michael Leitner

ii

Preamble

In this lecture course, a detailed account of the atomic scale in solids will be given. This is to be understood as the question of the arrangement of atoms, both of its statics and its dynamics. Specifically, it includes on the one hand a description of the crystalline state and the static deviations from it, such as point defects and disorder, and on the other hand a treatment of oscillatory and diffusive dynamics. As the positions of the atoms are the principal degrees of freedom considered here, any issues of the electronic state appear only indirectly via the potentials the atoms move in, and will not be discussed here.

Literature

- Fundaments of solid-state physics:

    - N. W. Ashcroft & N. D. Mermin: Solid State Physics, De Gruyter Oldenbourg (2012)
    - H. Ibach & H. Lüth: Festkörperphysik, Springer-Verlag (2009)
    - Ch. Kittel: Introduction to Solid State Physics, Wiley (2018)
    - R. Gross & A. Marx: Festkörperphysik, De Gruyter (2018)
    - U. Rössler: Solid State Theory: An Introduction, Springer-Verlag (2009)

- Statistical physics:

    - F. Schwabl: Statistische Mechanik, Springer-Verlag (2006)

- Classical metal physics:

    - G. Gottstein: Physikalische Grundlagen der Metallkunde, Springer-Verlag (2007)
    - P. Haasen: Physikalische Metallkunde, Springer-Verlag (2013)

- Classical solid-state chemistry:

    - J. Maier: Festkörper — Fehler und Funktion, Springer-Verlag (2000)

- Atomic aspects of solids:

    - M. T. Dove: Structure and Dynamics: An Atomic View of Materials, Oxford University Press (2003)

- Specialized aspects:

    - W. Borchardt-Ott, H. Sowa: Kristallographie. Eine Einführung für Naturwissenschaftler, Springer Spektrum (2013)
    - B. Fultz: Phase Transitions in Materials, Cambridge University Press (2014)
    - D. A. Porter & K. E. Easterling: Transformations in Metals and Alloys, Routledge (2009)

- R. J. D. Tilley: Defects in Solids, John Wiley & Sons (2008)

- A. M. Kosevich: The Crystal Lattice. Phonons, Solitons, Dislocations, Superlattices, Wiley-VCH (2005)

- H. Mehrer: Diffusion in Solids. Fundamentals, Methods, Materials, Diffusion-Controlled Processes, Springer-Verlag (2009)

- W. J. Moore: Seven Solid States, W. J. Benjamin, Inc. (1967)

- Internet resources:

  - Crystal lattice structures — definitions (and sketches) of important types of ordered compounds
    `https://homepage.univie.ac.at/michael.leitner/lattice/`.

Chapter A

Crystals

This chapter will present the fundamental concepts of the crystalline state, which in general is the framework appropriate for the atomic scale of solids. Also, it will consider the deviations from this idealized case, which are instrumental in determining the properties of real-world materials.

A.1 Symmetries

The distinguishing feature of crystals is the symmetries they display, which will be covered here. Fundamentally, this corresponds to the mathematical concept of groups, which will be the starting point.

A.1.1 General groups

A group is a set of elements $g \in G$ together with a binary operation $\circ : G \times G \to G$ that fulfill

- closedness: If $g_1 \in G$ and $g_2 \in G$ then $g_1 \circ g_2 \in G$.

- identity: $\exists e \in G : \forall g \in G$ we have $g \circ e = e \circ g = g$. This identity element is unique.

- inverse element: $\forall g \in G \, \exists g^{-1} \in G : g \circ g^{-1} = g^{-1} \circ g = e$. For a given element g, also the inverse element is unique.

- associativity: $\forall g_1, g_2, g_3 \in G : (g_1 \circ g_2) \circ g_3 = g_1 \circ (g_2 \circ g_3)$

If in addition $\forall g_1, g_2 \in G$ we have $g_1 \circ g_2 = g_2 \circ g_1$ then G is called commutative or Abelian group. If there is a subset $G' \subseteq G$ such that G' also fulfills the group axioms, then G' is called subgroup of G.

A.1.2   Symmetry groups

Crystallography is concerned mainly with spatial symmetries, which are isometric transformations of space (conserving lengths of vectors and relative angles). Let g be a transformation

$$\vec{x} \mapsto \vec{y} = g(\vec{x}). \tag{A.1.1}$$

For two transformations g_1 and g_2 also $g_3 = g_2 \circ g_1$ is a transformation defined by

$$g_3(\vec{x}) = g_2\big(g_1(\vec{x})\big). \tag{A.1.2}$$

It is easy to see that with respect to this function composition, the set of all isometric transformations of space is a group, which is called the Euclidean group.

For a given system, symmetries are such transformations g such that for any spatially varying quantity $f(\vec{x})$ we have $f(\vec{x}) = f\big(g(\vec{x})\big)$. For instance, $f(\vec{x})$ could be the electron density of the system. To see that those symmetry operations form a subgroup of the Euclidean group observe closedness: with $\vec{y} = g_1(\vec{x})$ we have $f\big(g_3(\vec{x})\big) = f\big(g_2 g_1(\vec{x})\big) = f\big(g_2(\vec{y})\big) = f(\vec{y}) = f\big(g_1(\vec{x})\big) = f(\vec{x})$, i.e. g_3 is also a symmetry. The identity element is the function $e : \vec{x} \mapsto \vec{y} = e(\vec{x}) = \vec{x}$, also the inverse elements exist as the inverse isometric transformations.

A.1.3   Point groups

Point groups are made up of symmetries that leave (at least) one point in space fixed. Such symmetries can be described by matrices according to $g(\vec{x}) = \mathbf{M} \cdot \vec{x}$ (matrix-vector product). In this description, the fixed point is the origin, and $\mathbf{M}$ is an orthogonal matrix ($\mathbf{M}^{\top}\mathbf{M} = \mathbf{M}\mathbf{M}^{\top} = \mathbb{1}$).

In three dimensions, apart from the trivial identity all possible symmetries can be classified into the following categories:

i. Inversion
$\mathbf{M} = \begin{pmatrix} -1 & 0 & 0 \\ 0 & -1 & 0 \\ 0 & 0 & -1 \end{pmatrix}, \quad \mathbf{M} \cdot \mathbf{M} = \mathbb{1}$

ii. Reflection about mirror plane
e.g. x-y-plane: $\mathbf{M} = \begin{pmatrix} 1 & 0 & 0 \\ 0 & 1 & 0 \\ 0 & 0 & -1 \end{pmatrix}, \quad \mathbf{M} \cdot \mathbf{M} = \mathbb{1}$

iii. Rotation through $\alpha = \frac{m}{n} 2\pi$ about some axis
For the special choice of the rotation axis lying along z: $\mathbf{M} = \begin{pmatrix} \cos\alpha & -\sin\alpha & 0 \\ \sin\alpha & \cos\alpha & 0 \\ 0 & 0 & 1 \end{pmatrix}$
n-fold application gives the identity: $\mathbf{M}^n = \mathbb{1}$

iv. Rotation-reflection
Consists of a rotation followed by a reflection about the plane orthogonal to the rotation axis. This can equivalently be seen as a rotation-inversion operation about an angle increased by π.

Only rotations (iii) can result from modifying the identity continuously, thereby corresponding to physically doable manipulations (*rigid motions*). Their matrices have a determinant of $+1$, and they are called *proper* operations. All other operations (apart from the identity) have a determinant of -1 and are called *improper* operations.

Neumann's principle says that any physical property of a crystal must obey all the crystal's symmetries, specifically conform to the point group. For instance, if a crystal has cubic symmetry, then also the elasticity constants have to display cubic symmetry.

Point groups consisting only of proper operations are called *enantiomorphic*: they conserve the handedness of the coordinate system and can therefore support chiral structures. Point groups that leave more than one point fixed are called *polar*. As a consequence of Neumann's principle, for instance only crystals with polar point groups can display pyroelectricity, only crystals lacking inversion symmetry can display piezoelectricity, and only crystals with enantiomorphic point groups can display optical activity (rotation of polarisation).

There is an unlimited number of point groups (e.g. the point groups of prismae with regular n-gons as base for all n). However, spatial periodicity (discrete translation symmetry) is only compatible with $n \in \{2, 3, 4, 6\}$ for rotation(-inversion/reflection) axes, and equal restrictions hold for the number and arrangement of mirror planes, leading to 32 different crystallographic point groups, of which 11 are enantiomorphic, 11 other are centrosymmetric (as inversion is obviously incompatible with handedness) and 10 polar (drawn from the non-centrosymmetric point groups). Here point groups that differ only by a rotated coordinate system are considered equal.

A crystal is said to have a given point group if there is a point within the unit cell so thatall the point group's symmetries are fulfilled with respect to this point, and if there is no larger such point group.

A.1.4 Translation groups

The spatial periodicity that is the defining property of crystals leads to translation symmetries: If all of

$$g_1(\vec{x}) = \vec{x} + \vec{a}_1 \qquad\qquad\qquad (A.1.3a)$$
$$g_2(\vec{x}) = \vec{x} + \vec{a}_2 \qquad\qquad\qquad (A.1.3b)$$
$$g_3(\vec{x}) = \vec{x} + \vec{a}_3 \qquad\qquad\qquad (A.1.3c)$$

are symmetries, then $g(\vec{x}) = \vec{x} + n_1\vec{a}_1 + n_2\vec{a}_2 + n_3\vec{a}_3$ is a symmetry $\forall n_i \in \mathbb{Z}$. For linearly independent $\vec{a}_i$, the set of vectors $\Lambda = \{\sum_{i=1}^{3} n_i\vec{a}_i | n_i \in \mathbb{Z}\}$ are the *Bravais lattice* of the crystal. There is a unique densest set Λ (corresponding to the primitive unit cell), while the lattice vectors $\vec{a}_i$ are not uniquely defined, i.e. different choices of $\vec{a}_i$ can result in the same Λ.

A.1.5   Space groups

The transformation group that includes all symmetries of a crystal is called space group S. The point group P and the translation group Λ are subgroups of the space group. Every element $g \in S$ can be written as the composition of an operation that leaves (at least) one point fixed and a translation:

$$g(\vec{x}) = \mathbf{M} \cdot \vec{x} + \vec{d} \Leftrightarrow g = g_{\vec{d}} \circ g_{\mathbf{M}} \tag{A.1.4}$$

Space groups that have only elements $g = g_{\vec{d}} \circ g_{\mathbf{M}}$ with $g_{\vec{d}} \in \Lambda$ and $g_{\mathbf{M}} \in P$ are called *symmorphic*.

Non-symmorphic space groups result if the symmetries include

- screw axes: rotation around an axis followed by translation along this axis, with $g_{\vec{d}} \notin \Lambda$ and $g_{\mathbf{M}} \notin P$, or

- glide planes: reflection about a plane followed by translation along a vector in this plane, with $g_{\vec{d}} \notin \Lambda$ and $g_{\mathbf{M}} \notin P$

There are 230 qualitatively different crystallographic space groups in three-dimensional space. Specifically, in this classification two space groups S_1 and S_2 are considered equivalent if they differ only by an orientation-preserving affine transformation of space f, that is, if there is an $f(\vec{x}) = \mathbf{N} \cdot \vec{x} + \vec{s}$ with $\det(\mathbf{N}) > 0$ so that for all $g_1 \in S_1$ there is a $g_2 \in S_2$ with $g_2 = f \circ g_1$. For instance, f can be an arbitrary orientation with isotropic scaling, or, in the case of lower-symmetry groups, also anisotropic scaling and shearing. In contrast, when the condition $\det(\mathbf{N}) > 0$ is dropped, there are only 219 so-called affine space groups in three dimensions. Thus, there are 11 pairs of crystallographic space groups that differ only by an inversion, with the simplest example of the tetragonal space groups $P4_1$ and $P4_3$, both consisting, apart from the translation group, only of a fourfold screw axis along z, but with a translation either along $(0, 0, 1/4)$ or $(0, 0, -1/4)$ for clockwise rotation by $90°$. Those are the so-called 11 enantiomorphic pairs, constituting the 22 chiral space groups.

There are 92 centrosymmetric space groups, that is, those that possess a point of inversion. Of course, the chiral space groups do not possess inversion symmetry. The chiral space groups (that have a notion of handedness already in the space group operations) together with 43 other space groups make up the 65 so-called Sohncke groups (sometimes also called enantiomorphic space groups), which are defined as including only proper operations. Thus, these are the groups that can support chiral crystals.

Of the 230 crystallographic space groups 73 are symmorphic. The space groups of Bravais lattices (i.e., when the space group has the highest symmetry compatible with a given translation group) are always symmorphic. Further, they always include inversion symmetry.

A.1.6   Bravais lattices and crystal systems

Point symmetry groups are commonly illustrated in the following way: A unit sphere S^2 is imagined, symbols for rotation(-inversion/reflection) axes are drawn at the corresponding positions, and great circles are drawn in full lines where mirror planes intersect. The upper hemisphere is then projected onto the plane through the equator via a stereographic projection from the south pole at $(0,0,-1)$:

$$(x,y,z) \in S^2 \mapsto (x,y) \cdot \frac{1}{z+1} \in \mathbb{R}^2 \tag{A.1.5}$$

The degree of rotation axes is given by the rotation symmetry of the symbols, and additional inversions/reflections are indicated as additional decorations. The presence of inversion symmetry is denoted by a small circle at the centre, and in the absence of a horizontal mirror plane the equator is drawn dashed.

Table A.1 illustrates the 14 distinct Bravais lattices in three dimensions, i.e., the different symmetry groups the translation group Λ can conform to. Specifically, they are classified into 7 *crystal systems* according to conditions fulfilled by the sides a,b,c and angles α,β,γ of the space-filling parallelepipeds[1]. For some of those systems, it is possible to add *centring operations*, i.e., additional translation operations, that are compatible to the imposed symmetry. Not all of those centring options lead to new lattices, however, e.g. the face-centred tetragonal lattice is equal to the body-centred tetragonal lattice with half the volume (analogous for base-centred and primitive), while for instance adding a base-centring to the cubic lattice breaks cubic symmetry.

The point group of highest symmetry for each crystal system is given in stereographic projection, where the pole of the projection lies in the vertical direction, apart for the monoclinic system. The axes along the body diagonal in the highest cubic symmetry are six-fold rotation-reflection axes (corresponding to a three-fold rotation when applied repeatedly). The crystal *basis* (the motif replicated by the translations) can have lower symmetry, which will lower the point group symmetry of the crystal. The number of such subgroups (including the given group of highest symmetry) there exist in each crystal system that are not also part of a crystal system of lower symmetry is also given. Note that, for instance, adding a motif with tetragonal symmetry to a Bravais lattice with cubic symmetry will result in a crystal with only tetragonal symmetry.[2]

The order of crystal systems is *triclinic* $\subseteq$ *monoclinic* $\subseteq$ *orthorhombic* $\subseteq$ *tetragonal* $\subseteq$ *cubic*, *monoclinic* $\subseteq$ *trigonal* $\subseteq$ *cubic*, *trigonal* $\subseteq$ *hexagonal* and *orthorhombic* $\subseteq$ *hexagonal*, understood as relations fulfilled by the highest-symmetry point group of the respective crystal systems.

---

[1]Apart for the hexagonal system, where a hexagonal prism is used to better illustrate the six-fold symmetry

[2]And for generic interaction potentials, a tetragonal basis would be expected to perturb the ground-state Bravais lattice away from *exact* cubic symmetry.

	7 crystal systems	primitive	face-cent.	body-cent.	base-cent.	32 point groups
triclinic						2 subgroups
monoclinic						$\alpha = \gamma = 90°$ 3 subgroups
orthorhombic						$\alpha = \beta = \gamma = 90°$ 3 subgroups
trigonal						$a = b = c$ $\alpha = \beta = \gamma$ 5 subgroups
hexagonal						$a = b$ $\alpha = \beta = 90°$ $\gamma = 60°$ 7 subgroups
tetragonal						$a = b$ $\alpha = \beta = \gamma = 90°$ 7 subgroups
cubic						$a = b = c$ $\alpha = \beta = \gamma = 90°$ 5 subgroups
	7 crystal systems		14 Bravais lattices			32 point groups
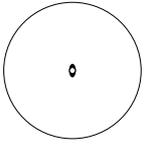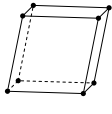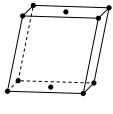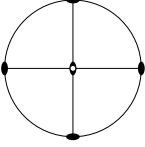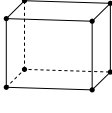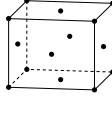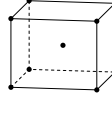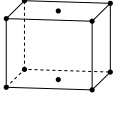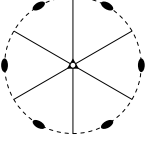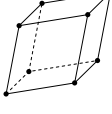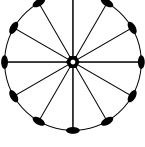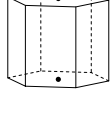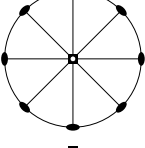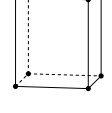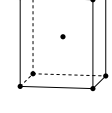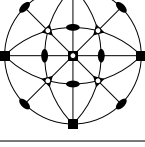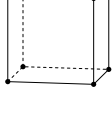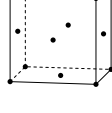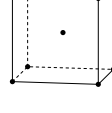
Table A.1: Crystal systems, Bravais lattices and point symmetries

A.1.7 Positions within the unit cell

For a given space group, locations within the unit cell can be classified into *general* and *special positions*. General positions x are those that are not invariant under any symmetry operation (apart from the identity), while for special positions there are some non-trivial operations that map them onto themselves. For instance, the centre of inversion is a special position, as well as all positions along rotation axes and on mirror planes.

The *multiplicity* of a given position is the number of positions within one unit cell that are obtained by applying all symmetry operations (and also the centring operations — so that, e.g., every position in a face-centred spacegroup has a least a multiplicity of 4). Such sets of positions are said to be related by symmetry. The multiplicity of special positions is a divisor of the multiplicity of the general positions, which in symmorphic groups is equal to the number of point group operations times the number of centring operations.

The locations of special positions within the unit cell are restricted, so that their location can be specified by at most two real parameters (if they are constrained to a mirror plane; only one if constrained to the intersection of two planes or to an axis, and zero degrees of freedom for even higher symmetries). For a given space group, the different special positions are catalogued, sorted and denoted by letters, where 'a' corresponds to the highest symmetry (there is no consistent way to do that for all space groups, therefore this nomenclature of so-called *Wyckoff positions* has to be looked up, if necessary). Often also the multiplicity is given, for instance in a face-centred cubic lattice the atoms sit at the special positions (4a) and in the diamond lattice at (8a). The highest-letter Wyckoff position[3] is the general site with generic position, meaning that its location within the unit cell is specified by three real parameters, e.g. coordinates with respect to the lattice vectors. Its multiplicity is the number of elements of the quotient group of the space group by the (uncentered) translation lattice.

A.2 Crystal structures

For the purposes of this lecture, atoms can be considered as having an ionic core that is made up of the positive nucleus and filled inner shells. These inner shells are spherical, and essentially impenetrable, as due to the Pauli exclusion principle an overlap of the inner shells of distinct atoms would cost a high amount of energy. The remaining atoms mediate the binding of the solid by metallic or covalent mechanisms, both of which tend to increase the valence orbital overlaps. The same holds for the Coulomb interaction in ionic crystals. As a consequence, the ground-state configuration follows as the optimal compromise between the inner shell repulsion and the Coulomb or valence-mediated attraction. For this reason, assigning some radius to a given element (depending on the situation there are sets of ionic or covalent radii) and modelling structures as being composed of hard spheres gives in quite a number of cases surprisingly good results.

---

[3]Space group 47 (Pmmm) has with 27 Wyckoff positions the largest number, here the general position is denoted by α or A.

Important concepts in this respect are the *volume filling fraction*, which corresponds to the relative part of space that is covered by such non-overlapping spheres, and the *coordination number Z*, which is the number of neighbouring atoms a given atom touches when the lattice constants are reduced to the minimal value.

A.2.1   Elemental systems on Bravais lattices

A.2.1.1   Face-centred cubic

The face-centred cubic (fcc) lattice is one of the most important crystal structures. The atoms occupy the (4a) positions of the $Fm\bar{3}m$ space group. As a close-packed structure (see the discussion at hexagonal close-packed and related structures), it has a volume filling fraction of $\pi/\sqrt{18} \approx 0.7405$ and a coordination number of $Z = 12$. The largest holes within such a close-packing of spheres are the octahedral sites at (4b), situated at $(1/2, 1/2, 1/2)$ and positions related via face-centring, which can hold a smaller sphere of radius $r_o = (\sqrt{2} - 1)R \approx 0.414R$ where $R = a/\sqrt{8}$ is the radius of the stacked spheres, and the tetrahedral sites at (8c), situated at $(1/4, 1/4, 1/4)$ and $(3/4, 3/4, 3/4)$ and positions related via face-centring, which can hold a sphere of radius $r_t = (\sqrt{6}/2 - 1)R \approx 0.225R$. These *interstitial* sites are candidates for inserting additional atoms into the structure.

A large number of metals, especially from the late transition groups over the noble metals, Al and Pb crystallize in this structure, as well as most noble gases. Lattice constants (i.e., the length of the cube edge) vary broadly from 3.6 Å for Co to 5.0 Å for Pb.

Its *Strukturbericht* designation is A1, and its prototype is Cu.

A.2.1.2   Body-centred cubic

This is another crystal structure that is prominent in metals. It is the main structure for the alkali metals and the transition metals of group 5B and 6B, as well as iron. The atoms occupy the (2a) positions in the $Im\bar{3}m$ space group. For such a structure made up of touching spheres the largest holes are at the tetrahedral sites at (12d), situated at $(0, 1/4, 1/2)$ and related positions, and can hold spheres of radius $r_t = (\sqrt{5/3} - 1)R \approx 0.291R$ with the radius of the stacked spheres $R = a\sqrt{3}/4$. For discussion below also the (6b) octahedral sites at $(0, 1/2, 0)$, $(1/2, 1/2, 0)$ and related positions shall be mentioned. Note that, in contrast to the fcc case, these interstitial sites do not display cubic symmetry (i.e., the tetrahedra and octahedra of near neighbours, after which the sites are named, are not regular).

Even though its volume fill fraction of $\pi\sqrt{3}/8 \approx 0.6802$ and low coordination number of $Z = 8$ seem to put this structure in metals at a disadvantage compared to close-packed structures, the distance to the six second-nearest neighbours along the cube edges is only 14% longer than to the eight nearest neighbours along the body diagonal, so that, given the right electronic configuration, to all of those

fourteen neighbours sizeable binding contributions can be expected. In fact, the bcc transition metals such as W have significantly higher melting temperatures than their neighbours. Further, in a number of systems (predominantly in the early transition metals) one observes a transition from a low-temperature close-packed structure to a high-temperature bcc phase. This is thought to be due to the increased vibrational entropy of the bcc phase.

Lattice constants are in the region of 2.9 Å (Fe) and 3.3 Å (Ta) for the transition metals, while for the alkali metals they increase up to 6.0 Å for Cs. The *Strukturbericht* designation of the bcc structure is A2, and its prototype is W.

A.2.1.3 Further examples

There is only a small number of elements that crystallize on a Bravais lattice, but neither in the fcc nor bcc structure. These include the α-phase of Po with the primitive cubic Bravais lattice (*Strukturbericht* A_h), and the high-temperature β-Po and Hg with the trigonal Bravais lattice. Note that the trigonal lattice results from the simple cubic lattice by stretching or compressing it along a body diagonal. For a specific stretching value, the fcc lattice results, while bcc results from a specific compression. In this sense, β-Po can be seen as slightly distorted bcc (which in the *Strukturbericht* is known as A_i), Hg as equally distorted fcc (A10). Note that while the A7 structure with prototype As (also shown by Sb and Bi) has a two-atom basis on the trigonal lattice, it can also be seen as primitive cubic lattice weakly distorted along a body diagonal, with the atoms alternatingly displaced along this dimension. Further, In crystallizes in the body-centred tetragonal lattice, which can also be seen as an fcc system where one cube edge is elongated by 8%.

A.2.2 Non-Bravais elemental systems

A.2.2.1 Close-packed structures

Consider a sheet of hexagonally arranged, touching spheres. This is a two-dimensional Bravais lattice, spanned by $\vec{a}_1 = a(1,0,0)$ and $\vec{a}_2 = a(-1/2, \sqrt{3}/2, 0)$. The gaps between these spheres do not form a Bravais-lattice, however: Their lattice has two sites per cell at $(\vec{a}_1 + 2\vec{a}_2)/3$ and $(2\vec{a}_1 + \vec{a}_2)/3$. Putting spheres directly over one those family of gaps, for instance at the positions $\vec{c}_1 = (\vec{a}_1 + 2\vec{a}_2)/3 + (0,0,c')$, gives again a sheet of hexagonally arranged spheres. Iterating this construction to infinity gives a Bravais lattice with $\vec{a}_3 = \vec{c}_1$. For the specific choice of $c' = \sqrt{2/3}a$ spheres in successive sheets are touching, and in this case the resulting Bravais lattice is just the face-centred cubic lattice in a primitive description with respect to a non-standard coordinate system. Projecting the sheets down to a basal plane, the lattice sites come to lie on three different two-dimensional Bravais lattices, corresponding to α, β and γ configurations, so that the fcc stacking corresponds to the $\alpha\beta\gamma\alpha\beta\gamma\dots$ sequence.

If, however, planes are displaced alternatingly by $\vec{c}_1$ and $\vec{c}_2$, leading to $\alpha\beta\alpha\beta\dots$ stacking, the third lattice vector is $\vec{a}_3 = (0,0,c)$ with $c = 2c'$. The corresponding

lattice belongs then to the hexagonal crystal system and is called the *hexagonal close-packed lattice* (hcp). Of course, the packing fraction depends only on c', so that for the specific choice of $c/a = 2c'/a = \sqrt{8/3} \approx 1.6330$ the packing fraction is equal to $\pi/\sqrt{18} \approx 0.7405$ as in the case of the fcc lattice, as well as its coordination number of $Z = 12$. Further, the sequence $\alpha\beta\gamma\alpha\beta\gamma\ldots$ gives the so-called *double hexagonal close-packed lattice* (dhcp), with four sites per unit cell. Note that both hcp and dhcp lattices have the same space group P6$_3$/mmc. With the standard convention of in-plane lattice vectors $\vec{a}_1$ and $\vec{a}_2$ enclosing a 120° angle and $\vec{a}_3$ perpendicular to them, the highest-symmetry Wyckoff positions are (2a) at $(0,0,0)$ and $(0,0,1/2)$, (2b) at $(0,0,1/4)$ and $(0,0,3/4)$, and (2c) at $(1/3,2/3,1/4)$ and $(2/3,1/3,3/4)$. In the hcp-lattice the (2c) sites are occupied, in the dhcp both (2a) (having local cubic symmetry) and (2c) (with hexagonal symmetry).

Both tetragonal and octahedral interstitial sites in the fcc lattice are between two close-packed planes. This motif is common to all close-packed structures, therefore also the interstitial sites are the same. Note also that only the Bravais case is potentially compatible with cubic symmetry, and therefore only in this case there is a reason that c should be exactly related to a.

A large number of elements crystallize in the hcp structure, predominantly early transition metals, rare earths, Be and Mg. In all these cases, $1.56 \leq c/a \leq 1.63$, i.e. the model of close-packed spheres is followed well. In contrast, Zn and Cd have c/a-values of 1.86 and 1.89, respectively, but still their structure is said to be hcp, as it has the same symmetry. The dhcp structure is displayed by the early Lanthanides from La through to Pm as well as the trans-uranium elements Am to Cf, and all of those have a c/a that agrees with the ideal one within 2.5%.

The *Strukturbericht* designation of hcp and dhcp is A3 and A3', respectively, and their prototypes are Mg and αLa.

A.2.2.2   Tetrahedrically coordinated structures

The sp^3-hybridisation of C corresponds to a local tetragonal coordination, which is fulfilled by the *diamond* structure: It consists of two fcc lattices that are displaced by a quarter of a cube diagonal. Equally, it can be obtained by taking a four-atom supercell of the bcc lattice and removing two of those atoms. Therefore, its coordination number as well as its packing fraction are half of the bcc packing values, which demonstrates that for covalently bound crystals dense packing is of no importance.

The two sites in this structure are related by symmetry, that is, they are the (8a) sites in the Fd$\bar{3}$m space group. C, Si, Ge and Sn, i.e. all elements in group IV apart from Pb, display this structure (C and Sn also display different structures). The prototype is the diamond modification of C and the *Strukturbericht* designation is A4.

Just as a tetrahedrically coordinated structure can be obtained from the close-packed fcc lattice by translating it so that the sites of the copy fall into tetrahedral voids between the sites of the original lattice, the same can be done for any close-packed lattice by translating it along the normal of the close-packed planes. Taking

the hcp lattice as original lattice, the resulting structure is called *lonsdaleite* (hexagonal diamond). It occurs as a modification of C and Si, and it has four atoms per unit cells. Note that, as with the non-fcc close-packed structures, there is no symmetry operations that relates the in-plane to the out-of-plane dimensions, so the tetrahedral coordination is in general fulfilled only to good accuracy, but not exactly. Just as in the case of the A7 structure discussed above, here symmetry does not constrain the atomic positions completely. Specifically, in addition to the unit cell dimensions a and c the atomic positions in the P6$_3$/mmc space group at the (4f) positions $(1/3, 2/3, z)$, $(2/3, 1/3, 1/2 + z)$, $(1/3, 2/3, 1/2 - z)$ and $(2/3, 1/3, -z)$ possess another degree of freedom z.

A.2.2.3 The graphite structure

The thermodynamical ground-state of C is hexagonal graphite. Its sp^2-hybridization corresponds to three-fold coordination, which is provided within planes of hexagonal honeycombs. These planes are then stacked in two-fold alternation, with a much larger separation between the planes than the within-plane nearest-neighbour distance, which leads to graphite being the element with the largest anisotropy in its properties. Again in the P6$_3$/mmc space group the atoms occupy the Wyckoff positions (2b) at $(0, 0, 1/4)$ and $(0, 0, 3/4)$, and (2c) at $(1/3, 2/3, 1/4)$ and $(2/3, 1/3, 3/4)$, thus the (2b) atoms have other (2b) neighbours in the planes above and below, while the (2c) atoms do not. Note that it is actually also possible that the planes are slightly buckled, with the (2c) atoms being shifted along the z-dimension with respect to the (2b) atoms, lowering the space group symmetry to P6$_3$mc. The prototype of hexagonal carbon is the graphite modification of C and the *Strukturbericht* designation is A9.

Further, specifically under mechanical load hexagonal graphite (also called α-graphite) can transform to the metastable form of rhombohedral graphite (β-graphite) with space group R$\bar{3}$m. The relation between those two forms is the same as between hcp and fcc: in β-graphite, the (optionally buckled) planes have a three-fold repetition compared to the two-fold repetition in α-graphite, so that each atom has exactly one out-of-plane neighbour either above or below it. The primitive unit cell has only two atoms, and it is actually the same structure as A7 discussed above, only with a much larger distortion along the body diagonal with respect to the simple cubic structure than in As, the prototype of A7.

A.2.2.4 Further remarks

Overall, there are about twenty more structures in the *Strukturbericht* A-series (denoting elemental systems), which will not be discussed here in detail. Only a few concluding remarks shall be given:

For B, local icosahedral configurations are energetically preferred. They do not fit well into a regular lattice, however, so that B has three common allotropes with large unit cells and approximately equal energies.

Mn is a quite flexible atom, it displays a large number of oxidation states. As

a consequence, its two low-temperature ambient-pressure phases (large cubic cells with 29 and 20 atoms, respectively) are rather described as intermetallic compounds, as Mn atoms on different Wyckoff positions have different electronic configurations. For instance, some of those sites host atoms that couple antiferromagnetically, while the atoms on other sites do not have a magnetic moment at all. At higher temperatures a body-centred tetragonal and finally a bcc phase follow, before sample eventually melts.

Also the actinides, specifically U, Np and Pu display complex phase diagrams with often large unit cells. Specifically Pu has six ambient-pressure phases, the reasons for which are not yet fully understood.

Finally also the non-metals can display very complicated structures, e.g. Se with a 64-atom primitive cell and S with a 32-atom primitive cell.

A.2.3   Ordered compounds

Systems consisting of more than one species of atoms can develop an ordered arrangement, where different sublattices (corresponding points in different primitive cells) are occupied by a different elemental make-up. Such systems are called *ordered compounds*. In the prototypical examples each sublattice is considered to be occupied by atoms of a single species, while, as will be seen later, in reality some degree of occupational disorder is to be expected. Ordered compounds are to be distinguished from *alloys*, which in the strict sense are multi-component systems without sublattices distinguished by elemental composition.

A principle that is often fulfilled by ordered compounds is to allow as much nearest-neighbour pairs of non-equal atoms as possible. This is because systems that crystallize as ordered compounds are those where such unlike pairs are energetically favoured, while systems where such pairs are disfavoured would display phase separation. This principle is fulfilled clearly for ionic compounds (see discussion there). Some important principles that determine ordered structures are discussed in the following, where the distinctions are not exclusive.

A.2.3.1   Superstructures

A large number of important ordered structures can be obtained by taking a fundamental lattice such as those discussed in A.2.1 and A.2.2, possibly enlarging the unit cell, and occupying the so-obtained sublattices by different elements.

For the simple cubic lattice A_h the so-obtained structure is the B1 structure, also called NaCl-structure due to its prototype. It consists of two face-centred cubic sublattices stacked into each other, so that each atom has six nearest neighbours of the other element. Analogously, taking the primitive orthorhombic Bravais lattice as fundamental lattices and occupying the lattices alternatingly gives the B24 structure with TlF as prototype.

Taking the body-centred cubic lattice as underlying lattice, a large variety of structures can be obtained in this way. Stacking four differently occupied face-

| | \multicolumn{4}{c}{Wyckoff position of F$\bar{4}$3m} | \multicolumn{3}{c}{nearest neighbours of} | prototype |
	(4a)	(4b)	(4c)	(4d)	A	B	C	
C1$_b$	A	B	C	-	4C	4C	4A+4B	MgAgAs
C1	A	-	C	C	8C		4A	CaF$_2$
L2$_1$	A	B	C	C	8C	8C	4A+4B	Cu$_2$MnAl
B32	A	B	A	B	4A+4B	4A+4B		NaTl
B2	A	A	B	B	8B	8A		CsCl
A2	A	A	A	A	8A			W

Table A.2: Superstructures of the A2 lattice, corresponding to sublattices at the Wyckoff positions (4a) at $(0,0,0)$, (4b) at $(1/2, 1/2, 1/2)$, (4c) at $(1/4, 1/4, 1/4)$, and (4d) at $(3/4, 3/4, 3/4)$ of the cubic face-centred space group F$\bar{4}$3m.

centred cubic sublattices inside each other gives the structures as defined in Table A.2. The L2$_1$ structure is the (full) Heusler structure with many intermetallic examples, and in analogy C1$_b$ is termed the half-Heusler structure. D0$_3$ with prototype Fe$_3$Al is actually the same structure as L2$_1$, but where the (4b) sublattice is also occupied by C. Note that the L2$_1$ structure can also be understood as an fcc lattice of A atoms, where the octahedral sites are filled by B and the tetrahedral sites by C. C1 is also called the fluorite structure and has predominantly covalently bound representatives (e.g., many fluorites and oxides). The two C sublattices in L2$_1$ and C1 together constitute a primitive cubic lattice, which also holds for the A and B sublattices in B2, while in B32 they constitute two diamond lattices. Thus, apart from C1$_b$ all those structures have higher symmetry than F$\bar{4}$3m.

The face-centred cubic lattice hosts triangles of nearest neighbours. Therefore there is no way to occupy neighbouring lattice sites alternatingly as in the case of B1 and B2. Here the most prominent example of a superstructure is the L1$_2$ structure with Cu$_3$Au as prototype, where the cube corners are occupied by one element and the cube faces by the other, so that each Au atom has 12 Cu neighbours, while each Cu atom has 4 Au and 8 Cu neighbours. This structure has the primitive cubic symmetry. Breaking this symmetry by stretching or compressing one of the three cube edges gives tetragonal symmetry and the L6$_0$ structure with prototype Ti$_3$Cu. Tetragonal symmetry also results when the (100) planes containing both elements are alternatingly shifted by half a face diagonal with respect to each other, giving the D0$_{22}$ structure with TiAl$_3$ as prototype, or the D0$_{23}$ structure with ZrAl$_3$ as prototype when pairs of two of those planes are shifted. Further, superstructures with AB stoichiometry are obtained when (100) planes are alternatingly occupied by different elements (L1$_0$ structure, prototype CuAu, tetragonal symmetry, each atom has 4 equal and 8 unequal nearest neighbours) or doing the same for (111) planes (L1$_1$ structure, prototype CuPt, trigonal symmetry, each atom has 6 equal and 6 unequal nearest neighbours).

For the tetrahedrically coordinated structures the B3 structure (also called zinc-blende structure, prototype ZnS) results from occupying the two fcc sublattices that make up the diamond lattice by different elements, analogously lonsdaleite's two hcp sublattices to get the B4 structure (wurtzite structure, with the corresponding modification of ZnS as prototype). These are the main structures for predominantly covalently bound group III-V semiconductors and insulators, where in both cases

each atom has 4 unequal neighbours.

Finally, by occupying alternating close-packed planes by different atoms the B_h structure (prototype WC) results from the hcp lattice, and the $B8_1$ structure (prototype NiAs) results from the dhcp lattice. Here each atom has 6 equal and 6 unequal neighbours with respect to the underlying close-packing, but actually for instance in the prototypical tungsten carbide $c/a \approx 0.98$, so that a more realistic view is that each atom has 6 close neighbours of opposite kind and 8 farther neighbours of the same kind. Occupying the close-packed planes in hcp (stacking $\alpha\beta\alpha\beta$) in a AABAAB-fashion gives the C7 structure (prototype MoS_2), and taking a close-packed structure with $\alpha\beta\gamma\beta\gamma$ stacking repetition and ABAAB occupation repetition gives the $D5_{13}$ structure with prototype Ni_2Al_3.

A.2.3.2 Structures by filling interstitial sites

Another way to derive ordered structures is to take a given simple structure and fill some interstitial sites by atoms of another kind. Interstitial compounds in the strict sense of the term, also call Hägg phases, are those where metallic atoms constitute an underlying structure and small atoms, such as H, B, C and N, fill interstitial sites. Characteristic for those compounds is a strict maximum content of the interstitial species (corresponding to a filling of all available sites), while the phases are often stable under some interstitial deficiencies. Due to the (mostly covalent) binding introduced by the interstitial species, in addition to the metallic binding on the host lattice, these compounds are often hard: for instance $Ta_{50+x}C_{50-x}$ is the solid with highest melting temperature of 3985 °C at a C deficiency of $x = 3$ and an existence region from $x = 0$ to 13. Its B1 structure can be seen as fcc where all octahedral sites are filled by the other element. Analogously, the B3 and C1 structures are just fcc structures with half or all of the tetrahedral sites filled, respectively, and the $B8_1$ structure is a hcp structure with all octahedral sites filled.

New structures obtained by filling interstitial sites are the C3 cuprite structure with prototype Ag_2O resulting from an fcc lattice where just two diagonally opposite tetrahedral sites are filled, which keeps cubic symmetry. Taking a B2 structure and filling the face centres (half of the octahedral sites) by a third element gives the $E2_1$ cubic perovskite structure with prototype $CaTiO_3$ displayed by many oxides. The larger Ca sites have 12-fold oxygen coordination, while the smaller Ti sites have only 6-fold oxygen coordination. Leaving the Ca sites empty gives the $D0_9$ structure with prototype α-ReO_3.

Taking a hexagonal close-packed structure and inserting a two-dimensional honeycomb lattice between every second pair of close-packed planes so that the inserted sites coincide with two thirds of the octahedral holes gives the $D0_5$ structure (BiI_3). Filling all octahedral sites on every second interstitial plane gives the C6 structure (prototype CdI_2, also called trigonal ω phase), while doing the same for the face-centred cubic structure gives the hexagonal C19 structure (with the elemental prototype α-Sm, but e.g. $CdCl_2$ as a more typical representative). In typical systems displaying those structures the inserted planes mediate a strong binding between their respective neighbours, while the binding between the planes with

the non-occupied holes is weak, leading to easy cleaving. On the other hand, reducing the distance between the weakly-bound planes in the trigonal ω structure to zero leads to a stacking of honeycomb planes and close-packed planes, which is called the hexagonal ω phase or C32 structure (prototype AlB_2), and which is rather described as primitive hexagonal lattice where the centres of all triangular prismae are occupied.

A.2.3.3 Coordination-maximizing structures

Specifically for metals, the Coulomb interaction between the conduction electrons and the ionic cores favours high densities of the electron gas, while the exact configuration of the atoms is only of secondary importance. This reasoning motivates the preference for dense packings. For elemental systems, the solutions to this problem are the comparatively simple close-packed structures. However, for systems composed of multiple elements with ionic cores of different sizes, a large variety of structures results. An underlying principle here is the maximization of the coordination numbers, motivated by the observation that high numbers of nearest neighbours per site exclude holes in the structure and therefore correspond to efficient packing, while the concept of an ionic core's size in a metal is not well defined. Structures that have only tetrahedral interstitial voids (i.e., where all larger voids are filled) are called *topologically close-packed* or *Frank-Kasper* phases. Note that the attribute "topological" shall imply some looseness on the order of 10% when counting the number of closest neighbours.

A prototypical example is the cubic A15 phase with prototype Cr_3Si. Here the Si atoms sit at the sites of a bcc lattice, and the Cr atoms occupy half of the tetrahedral voids, such that on a given face for instance the sites $(0, 1/2, 1/2 \pm 1/4)$ are occupied. In this way, Si has 12 Cr neighbours, while Cr has 4 Si neighbours and additionally 2 Cr neighbours about 10% nearer and 8 Cr neighbours about 10% farther, giving an effective coordination number of 14.

Another important class of topologically close-packed structures is the Laves family. Its cubic C15 member with prototype $MgCu_2$ has Mg on a diamond lattice and Cu on corner-sharing tetrahedra centred around the diamond lattice's tetrahedral voids, i.e., those empty sites that, if filled, would transform the diamond lattice to bcc. Mg consequently has 12 Cu neighbours and 4 Mg neighbours about 5% farther away, while Cu has 6 Mg neighbours and 6 additional Cu neighbours 15% nearer. This principle of filling the tetrahedrical voids within tetrahedrically coordinated underlying structures by corner-sharing tetrahedra can of course also be applied to the Lonsdaleite structure (with $\alpha\beta\alpha\beta$-stacking), giving the C14 structure with prototype $MgZn_2$, and to a structure with $\alpha\beta\alpha\gamma$-stacking, giving the C36 structure ($MgNi_2$). For those two hexagonal Laves phases the internal degrees of freedom are typically very close to the ideal ones.

The tetragonal $D8_b$ structure (also called σ-phase) with FeCr as prototype has a large technological relevance. As is common for intermetallic topologically close-packed structures, it is very brittle and therefore undesirable in steel metallurgy (sigma phase embrittlement). It has 30 atoms per cell on 5 inequivalent sites with coordination numbers 12, 14 and 15. Finally, the low-temperature α and β phases

of Mn (structures which are also displayed by multicomponent systems) can also be considered as topologically close-packed structures, with coordination numbers from 12 to 16.

A.2.3.4   Structures with preferred covalent configurations

For systems with significant covalent interactions, structures with characteristic local motifs can be preferred. This includes the large family of octahedron-based minerals, with many members among the oxides, sulfides, fluorides and chlorides:

The simplest such structure is $D0_9$ mentioned already above, which consists of corner-sharing ideal octahedra with another element at the octahedron centres. Tilting those octahedra gives the cubic $D0_2$ (prototype $CoAs_3$) skutterudite structure, where the Co atoms are still nearly ideally octahedrically coordinated to As, while As has additional to the two Co atoms also two As neighbours in approximately the same distance.

The cubic C2 pyrite structure (prototype FeS_2) can be derived from the C1 structure by shifting the S atoms from the tetrahedron sites within the Fe fcc lattice through the centre of one of the tetrahedron's triangular faces. In this way, the eight-fold coordination of Fe is broken down to a skewed octahedron, while S has now three Fe neighbours and in addition another S neighbour in approximately the same distance. In the C4 rutile structure (prototype TiO_2) the Ti atoms sit on a body-centred tetragonal lattice, and the O atoms are at the centres of the resulting Ti-triangles, so that Ti has 6 O neighbours in a stretched octahedral configuration, while O has 3 Ti neighbours.

The backbone of the cubic $H1_1$ spinel structure (prototype Al_2MgO_4) is a face-centred cubic lattice of O. One eighth of the tetrahedron sites are occupied by Mg, making up a diamond lattice, while Al occupies half of the octahedron sites so that it forms tetrahedra centred around the the fcc-tetrahedron voids not occupied by Mg. As a result, Mg is coordinated by a tetrahedron of O, Al by an octahedron of O, and O has one Mg and 3 Al as neighbours, where actually the distance to Mg is shorter due to a small distortion of the O fcc lattice.

As an example for crystal structures with a different defining local motif the B20 structure (prototype FeSi) shall be discussed. It conforms to the cubic $P2_13$ space group and has both elements on (4a) sites with different internal degrees of freedom. It can be considered as a NaCl-structure where the atoms are displaced along the body diagonals. For an ideal choice of internal parameters, each atom has 7 unlike neighbours and 6 like neighbours about 15% farther away.

A.2.3.5   Ionic compounds

In contrast to general systems, ionic systems are a special case where the resulting structure can be understood quite easily. The model is that the metallic constituents release an integral number of electrons, which are accepted by the non-metallic atoms. In itself, this costs energy, i.e., the ionization energy of the metal is in general higher than the binding energy of the electron at the non-metal,

so that for isolated atoms this would not happen. However, bringing the ions into contact releases Coulomb energy, leading to a positive binding energy.

Specifically the alkali halides, consisting of an alkali metal and a halogen in equiatomic fractions, provide a nice example. Here one electron is transferred, leading to noble gas configuration on both constituents. The resulting ions can be considered as charged soft spheres: at short distances, once their electron clouds penetrate each other, they experience a rapidly increasing repulsive potential due to the Pauli exclusion principle, while at larger distances the Coulomb interaction dominates.

Most of the alkali halides crystallize in the B1 structure, with the exception of CsCl, CsBr and CsI, which have the B2 structure. The remarkable fact is now that it is possible to assign an ionic radius to each element so that the lattice constants of 14 among the 20 compounds are predicted accurately within 2% by requiring cations and anions to touch. The remaining 6 compounds are those where the anions are so much larger than the cations that they would be nearly touching or actually overlapping. In fact, predicting the lattice constants of the systems that would have overlapping anions so that the anion pairs instead of the nearest-neighbour cation-anion-pairs touch again gives an agreement with measured lattice constants within 2%.

In the II-VI-compounds larger ratios between anion and cation radii occur, specifically for the Be-compounds and MgTe. These systems display the tetrahedrically coordinated B3 or B4 compounds: Even though the Coulomb energy at given nearest-neighbour distance (i.e., the Madelung constant) is significantly smaller for those structures than for B1 or B2, the lower coordination allows for smaller nearest-neighbour distances. Apart from those B3 and B4 systems, where the covalent nature of the binding begins to prevail, ionic radii can predict lattice constants equally well as in the case of the I-VII-compounds.

A.3   Point defects

In reality, materials deviate from the ideal crystal structures discussed in Section A.2. If the region of disturbance is confined to a compact domain, a mapping of atoms to lattice sites remains unambiguous. Such types of defect are called *point defects* or zero-dimensional defects. One- and two-dimensional defects, where a global assignment of atoms to lattice positions is not possible any more, will not be covered here.

Here isolated point defects will be discussed, where in some cases even questions of their qualitative properties are not yet settled. They can be naturally classified according to the number of atoms within a region that encompasses the defect, compared to the ideal number within this region. If an atom is missing, the defect is called single *vacancy* (or vacancy cluster for more missing atoms), if there is an additional atom, it is called *interstitial* atom (or cluster for multiple atoms). Compact defect configurations with the correct number of atoms are typically unstable and annihilate immediately, they are only realized as intermediate states during diffusion events (see there). In ordered compounds there is a third

possibility of *intrinsic* defect (i.e. defects that form as excitations of the ideal atomic arrangement due to thermodynamics, see below), where a site that should be occupied by an atom of element A is occupied by B. This type of defect is called *antisite*, and the wrong atom is called *anti-structure atom*. Impurities of foreign elements are a type of *extrinsic* defect (those that do not form spontaneously), they can be incorporated either as substitutional defect, where they occupy a regular lattice site, or as interstitials.

Obviously, an isolated point defect destroys translation symmetry. However, point group operations that have the position of the defect as fixed point are still possible. Therefore, the point symmetry is a distinctive feature of a defect. It depends on how the atoms in the vicinity of a point defect relax their position to accomodate the inserted or removed atom.

A.3.1   Formation energies, entropies, and volumes

The appropriate framework for discussing the energetics of intrinsic point defects are their formation energies[4]. They are defined as the (necessarily positive) energy differences between the unperturbed crystal and a crystal with a single point defect. The constraint of mass conservation in experiments introduces subtleties to this issue:

Consider first a calculational method that assumes periodic boundary conditions (i.e. no crystal surfaces) and that can compute the internal energy for systems composed of an arbitrary number of atoms. For simplicity, we restrict ourselves to the case of an elemental system on a Bravais lattice. Let E_{id}^N be the total internal energy for an ideal system with N atoms and observe that $E_{\text{id}}^N/N = E_{\text{id}}^1 = E_0$. If E_{vac}^M is the total internal energy for a system consisting of M atoms on $M+1$ sites (i.e. including one vacancy), then the vacancy formation energy follows as $E_{\text{vac}}^{\text{f}} = E_{\text{vac}}^M - M \cdot E_0$. Similarly the self-interstitial formation energy is given by $E_{\text{int}}^{\text{f}} = E_{\text{int}}^M - M \cdot E_0$, where E_{int}^M is the energy of a system of M atoms on $M-1$ sites.

In reality, however, any crystal is finite, therefore surface energy contributions have to be considered. In general, surfaces are not ideally flat, but display terraces where halflayers of atoms end. Further, also these terraces are not ideally linear, but have kinks, where half-columns of atoms end. The last atom of such a half-column is said to be in *Halbkristalllage*, as (for the Bravais case) it has exactly $Z/2$ occupied neighbouring sites and $Z/2$ unoccupied neighbouring sites. For short-range interactions, inserting an atom at such a special site does not change the surface contributions to the thermodynamics of the sample, which can be seen by observing that the number of atoms embedded in a surface layer, at a terrace, and at the kink is the same before and after inserting the last atom. Note that this is not the case when, for instance, adding an atom onto a complete layer.

---

[4]Note that the internal energy is the thermodynamic potential at fixed volume, while the enthalpy is the potential at fixed pressure. In a strict sense, formation *enthalpies* would be the relevant quantities, as experimentally a sample rarely has a fixed volume, but rather relaxes its volume under given external pressure. Still, I will call it sloppily formation *energy*, to be understood as the energy at the optimally relaxed volume, which is equal to the formation enthalpy at $p = 0$, which in turn is approximately equal to the enthalpy at ambient pressures due to the large bulk modulus of solids.

Experimentally, the vacancy formation energy can now be understood as removing an atom from the bulk and inserting it in *Halbkristalllage*, and the self-interstitial formation energy by removing it from there and squeezing it into the bulk. In a simple example where the internal energy of a crystal is given by nearest-neighbour pair potentials, the vacancy formation energy corresponds therefore to the breaking of $Z/2$ nearest-neighbour bonds.

Just as with energies, also the relaxed volume changes when a point defect is introduced, corresponding to its formation volume: $\Omega^{\mathrm{f}}_{\mathrm{vac}} = \Omega^{M}_{\mathrm{vac}} - M \cdot \Omega_0$, where Ω denotes the volume of smallest internal energy, equivalently for interstitials. The formation volume of point defects are in general positive, i.e. by removing an atom from the bulk the crystal shrinks not so much as to make up for the increase in volume when inserting the atom at the surface, leading to vacancy formation volumes of about $0.5\,\Omega_0$. This holds also for self-interstitials, the local strains give a crystal expansion that is typically larger than the atomic volume, giving formation volumes on the order of Ω_0, where these values are still subject to large uncertainties.

Finally, point defects also have an associated formation entropy, which means that the number of states within a given excitation energy can be different from the ideal structure. The most relevant contribution here is from vibrational excitation. For instance, the less tightly bound neighbours of a vacancy will experience lower restoring forces and thereby cover larger volumes of phase space at a given temperature. This would increase the entropy of a crystal with a vacancy over the value for the perfect crystal, corresponding to a positive entropies.

For ordered compounds the situation becomes more complicated. Here the requirement of atom number conservation together with fixed proportions of sites on the respective sublattices allow point defects to be generated only in combinations. As a consequence, only those combinations of point defects have well-defined formation energies, as will be discussed in detail below.

Extrinsic point defects can only be generated by particle exchange with the outside. As a consequence, their formation energies depend on a chemical potential that has to be defined in some way. For instance, a sensible choice for H interstitials is to compare the energy of the ideal crystal and a H_2 molecule with the situation when the two H atoms are dissolved.

A.3.2 Vacancies

The high symmetry that is generally displayed by metallic structures carries over to their vacancies. As a rule, when removing an atom from the bcc or fcc structure the full cubic point symmetry around the previous position of the atom is conserved (at least, this assumption is seldom questioned). This constrains the relaxations of the neighbouring atoms: for instance, as there are rotation axes along $\langle 100 \rangle$, $\langle 110 \rangle$, and $\langle 111 \rangle$, all atoms that are related by one of those directions to the vacant site (which includes the first three neighbour shells in bcc and the first two in fcc) can only relax longitudinally.

The same holds for simple ordered compounds such as B1 or B2. It also holds for

vacancies on the B-sublattice of an $L1_2$-system with A_3B-composition, as these sites display the full cubic symmetry. However, the A-sites have only tetragonal symmetry also in the ideal crystal, therefore A-vacancies cannot have higher symmetry. Analogously, the sites in the cubic B20 structure have only a trigonal point symmetry, therefore the relaxations are only weakly restricted by symmetry.

In non-metallic systems the situation can be more complicated. In the diamond lattice of Si, the sites have tetrahedral point group symmetry. Depending on the charge state of the vacancy (which is an additional parameter in non-metallic systems), it has different configurations as predicted by recent calculations and partially already known from experiment. For a doubly positively charged vacancy, tetrahedral symmetry is retained. For charge states +1 and 0, the two neighbour pairs of the vacancy are shifted outwards along $\langle 100 \rangle$, resulting in tetragonal symmetry. At charge state -1, the symmetry is still lowered to orthorhombic by different lengths of those two neighbour pairs (while their $\langle 011 \rangle$-orientation is kept). Finally, at charge -2, trigonal symmetry along $\langle 111 \rangle$ is predicted by starting again from the unrelaxed case and moving one neighbour of the vacancy halfways towards the vacancy, resulting in the so-called split-vacancy configuration.

Apart from cases such as the split-vacancy configuration, relaxations around vacancies are typically on the order of a few percent of the nearest-neighbour distances for the nearest neighbours. A priori, both inward as well as outward relaxations are possible. The relaxation distances decay rapidly with the distance from the defects. Macroscopic elasticity theory predicts a decay with r^{-2} at large r, converging to some value of volume change corresponding to the formation volume.

In elemental systems, the vacancy formation energies roughly scale with the melting temperature. Typical values are 0.6 eV for Al, 1.1 eV for Cu, and 3.4 eV for W. The relation between vacancy formation energy and melting temperature leads to the empirical rule of thumb of a vacancy concentration of about 10^{-4} per atom at the melting temperature.

In compounds with ionic character, an isolated vacancy necessarily has a charge. Therefore, in these systems there is a tendency for defects of opposite charge to appear in combination. In order to explain experimental vacancy concentrations, also for metals the existence of divacancies in equilibrium at high temperatures has been proposed since the 1970s, but only recently convincing counterevidence has been put forward (see discussion in A.5.1). Only in very non-equilibrium situations, such as in a nuclear reactor, irradiation-induced vacancies can condense to microvoids in order to reduce the internal surfaces.

A.3.3   Interstitials

When an additional atom is inserted into a structure, one could assume that it is accomodated in one of the voids between atoms imagined as touching spheres, as was discussed under the term "interstitial sites" in Section A.2. For small impurity elements such as H, B, C, and N, this is what actually happens, leading to the Hägg phases discussed above, where the lattice backbone is not much affected

by the occupation or non-occupation of a given interstitial site. However, for *self-interstitials*, where the excess atom is of the same element as those making up the lattice, the available space is typically too small, so that this picture is qualitatively not correct any more.

For structures of high symmetry such as bcc and fcc, often configurations that keep a symmetry axis are metastable. This means that they are local minima of the energy as function of the atomic positions. Here one can distinguish whether there is an atom at the point symmetry centre (which is then at an interstitial site) or there is no atom at the centre (which is then at a lattice site). As mentioned above, the first case is often realized for small impurities, for instance C in bcc-Fe occupies the octahedral sites (which, as discussed above, have actually only tetragonal symmetry) with large outward relaxations of the two nearest neighbours in $\langle 100 \rangle$ direction.

For self-interstitials, the excess atom typically shares a lattice site symmetrically with another atom, so that the point symmetry centre is at the lattice site. Such a configuration is called *dumbbell*. In fcc systems, the configuration with lowest energy is typically the $\langle 100 \rangle$-dumbbell with tetragonal symmetry. In bcc systems, it is generally the $\langle 111 \rangle$-dumbbell with trigonal symmetry (actually a crowdion, see below), with the important counter-example of α-Fe, where magnetic interactions favour the $\langle 110 \rangle$-dumbbell with orthorhombic symmetry.

As in the case of vacancies, for the diamond lattice with Si as example the situation is more complicated. Here calculations cannot resolve the energy differences between the low-symmetry $\langle 110 \rangle$-dumbbell and the "hexagonal" configuration (halfways between two tetrahedral sites, with a $\langle 111 \rangle$ rotation axis and trigonal symmetry), with the tetrahedral configuration closely following.

Due to the dense packing in metallic systems, a self-interstitial atom leads to large local strain in the lattice and has therefore a large formation energy, typically a few times the formation energy of a vacancy. This is the value predicted by calculations, while the corresponding small equilibrium defect concentrations render experimental determinations of the formation energy impossible. In fact, self-interstitials in metals are only relevant in irradiation studies. In more open structures such as the diamond lattice, the energy difference between vacancies and self-interstitials is smaller. While also here self-interstitials are much less numerous in equilibrium than vacancies, their small migration energies can make them relevant for diffusion (see the discussion in Sect. **??**).

In this context, also the *crowdion* shall be mentioned. Similar to a dumbbell, it has an axis of orientation, but in this case it is oriented along a close-packed direction (i.e. $\langle 110 \rangle$ in fcc and $\langle 111 \rangle$ in bcc). Because of the close-packing, the number of atoms with significant shifts in this direction is larger than in the dumbbell-case. It has been proposed as a means for very rapid diffusional motion along its axis. This is because there would be virtually no energy difference when the defect migrates, as the large extent of the moving column smooths the interactions with the non-moving neighbours. For bcc systems, this indeed seems to be the case. Around the 1970s, it was assumed to be active also in fcc systems in parts of the scientific community, although in recent times it has fallen out of favour.

A.3.4   Substitutional defects

The third type of point defects are substitutional defects, where a site is occupied by a wrong species of atom. Introducing impurities of comparable size as the constituent atoms into a system will in general lead to their being incorporated into the host lattice. Qualitatively, for aspects such as local relaxations and symmetry breaking the same holds as for vacancies. A quantitative definition of formation energies would require the choice of a reference state. As will be derived later, the temperature-dependent terminal solubility in phase diagrams directly gives the formation energies of these defects, and the wide variation of such solubilities in different systems and therefore of the formation energies can be rationalized in terms of chemical and geometrical compatibilities.

The empirical Hume-Rothery rules predict that solubilities are large if

- the atomic radii of solvent and solute do not differ much (a typical critical value is 15%)

- the solute has the same or higher valency than the solvent

- the electronegativities are comparable (otherwise intermetallic phases are formed)

- the crystal structure of pure solvent and solute are the same.

The latter two rules are relevant for the central regions of the phase diagram, which will be discussed later. For the case of small solute concentrations, where the image of isolated impurities is appropriate the former two are relevant.

In ordered compounds, placing atoms of a constituent species on a wrong sublattice gives another kind of substitutional defects. This case is discussed in the following.

A.3.5   Point defects in ordered compounds

Ordered compounds have at least two constituent species and at least two sublattices, each of which is ideally occupied by only one species. For simplicity we will assume in the following discussion a binary compound consisting of species A and B in ideally equiatomic composition with the corresponding sublattices α and β, each having one site per primitive cell, with the B1, B2, or B3 structures as exemplary representants.

In ordered compounds, three additional issues with respect to point defects compared to the case of elemental systems on Bravais lattices arise: First, there are substitutional point defects with intrinsic reasons, namely when an A and a B atom exchange their sites as a thermal excitation. Second, when deviating from stoichiometry extrinsic point defects comprising only constituent species result. And finally, the fixed relation of sublattice sites together with atom number conservation leads to thermal point defects only appearing in combination.

Substitutional point defects comprising constituent species use the following nomenclature: a B atom on the α sublattice is called an *antisite* on the α sublattice, or an α-antisite in short (for the case of more than two constituent species it would be necessary to additionally specify the kind of participating atom). The atom that sits on the wrong sublattice is called *anti-structure atom*.

The following thermal excitations of the ideal site occupations are possible:[5] First, two unequal atoms can exchange positions, leading to an antisite pair. Second, the crystal can be enlarged by one unit cell, leading to a vacancy pair, which is also called a Schottky defect. Finally, it is possible that after creating a vacancy pair, an A atom fills the β vacancy, resulting in two α vacancies and an A atom on the wrong sublattice (i.e., a β antisite). This configuration is called a triple defect, in this case an A-triple defect. Of course, the various kinds of interstitials would enlarge this zoo of excitations even more, but for simplicity, and as their number in typical metallic systems is very low, we did not consider them here. Also, for the case of a larger number of sublattice sites per unit cell the corresponding number of vacancies would have to be generated at the same time, and the excitations corresponding to triple defects in the case considered here would be more complicated.

The four excitations considered above (antisite pairs, vacancy pairs, A- and B-triple defects) have well-defined formation energies. However, these energies are not independent: generating an A- and a B-triple defect leads to the same situation as two vacancy pairs and one antisite pair, therefore the respective formation energies have to fulfill the corresponding equation. This can also be seen by counting the sites: let n_α^A, n_α^B, and n_α^V be the numbers of correctly occupied α sites, α antisites, and α vacancies, respectively, and analogously for β. These six variables are subject to three boundary conditions $n_\alpha^A + n_\beta^A = n^A$ (conservation of A atoms), the analogous expression for B atoms, and $n_\alpha^A + n_\alpha^B + n_\alpha^V = n_\beta^A + n_\beta^B + n_\beta^V$ (creation of α and β sites only in combination), leading to three degrees of freedom.

As the numbers of the four different point defects (vacancies and antisites on α and β) cannot be varied independently, their formation energies are not well-defined. An elegant way to treat the problem of point defects in ordered compounds is to consider the grand-canonical ensemble, which in general implies that particle numbers can vary and that the internal energy of a given state is modified by a term linear in the particle numbers, where the proportionality constants are called chemical potentials.

For the present case, the experimental situation of a canonical ensemble with fixed particle numbers and free numbers of sublattice sites (which can vary by enlarging the crystal and generating vacancies in the interior) is mapped to a grand-canonical ensemble of fixed number of sublattice sites and varying particle numbers (for a discussion of these two approaches see A.5.1). As the ideal configuration is the reference state, the internal energy does not change by enlarging the crystal by one unit cell. Therefore the chemical potentials for the two species have to fulfill $\mu_A = -\mu_B =: \mu$. This leads to the so-called effective

---

[5]Note that even though these excitations are generated by some sequence of atomic movements at some position and that therefore the participating point defects are initially spatially conjoint, with time they will become separated. These separated states are the ones considered here.

	FeAl				NiAl			
	E_α^{v}	E_β^{v}	E_α^{Al}	E_β^{Fe}	E_α^{v}	E_β^{v}	E_α^{Al}	E_β^{Ni}
Al-poor	1.56	2.96	1.98	0	1.11	1.60	3.10	0
stoichiometric	1.06	3.46	0.99	0.99	0.74	1.97	2.36	0.74
Al-rich	0.56	3.96	0	1.98	0	2.71	0.88	2.22

Table A.3: Effective formation energies in units of eV for B2 FeAl and NiAl. Ideally, the transition metal occupies the α-sublattice and Al the β-sublattice.

formation energies

$$E_\alpha^{\mathrm{v}}(\mu) = E_\alpha^{\mathrm{v}}(0) - \mu \tag{A.3.1a}$$

$$E_\alpha^{\mathrm{B}}(\mu) = E_\alpha^{\mathrm{B}}(0) - 2\mu \tag{A.3.1b}$$

$$E_\beta^{\mathrm{v}}(\mu) = E_\beta^{\mathrm{v}}(0) + \mu \tag{A.3.1c}$$

$$E_\beta^{\mathrm{A}}(\mu) = E_\beta^{\mathrm{A}}(0) + 2\mu \tag{A.3.1d}$$

having one degree of freedom μ.

As will be shown in A.5.1, for fixed composition the concentrations of the four point defect species vary at low temperature according to

$$c_X \propto \mathrm{e}^{-E_\mathrm{X}/k_\mathrm{B}T} . \tag{A.3.2}$$

For a general non-stoichiometric composition, one of the four considered point defects is the *constitutional defect*, i.e. the defect that exists at non-vanishing concentration down to $T = 0$ and that accomodates the deviation from stoichiometry. For the above equation to be fulfilled, its effective formation energy has to vanish. This condition, together with the obvious condition that no effective formation energy can be negative, specifies μ unambiguously and allows to determine which defect is the constitutional defect for a given composition from three independent formation energies of thermal excitations. On the other hand, in the stoichiometric case at least two different point defects have to be generated in combination as thermal excitations, which implies choosing μ so that two effective formation energies are equal and lower than the other two.

These concepts are exemplified by the cases of B2-NiAl and FeAl according to calculations of formation energies. Table A.3 shows that an excess of the transition metal is always accomodated by antisites, which holds also for Al-rich FeAl, while NiAl displays constitutional vacancies in this case. In the stoichiometric case, the principal thermal excitations are Ni triple defects for NiAl and antisite-pairs for FeAl (although Fe triple defects are only barely more expensive), while transition metal triple defects are the principal thermal excitation in both transition metal-rich cases, where antisites on the Al sublattice are generated in addition to the constitutional antisites. The Al-rich cases differ again, here FeAl shows antisite annihilation (where a vacancy pair is generated, one of which is successively filled by a constitutional Fe anti-structure atom, giving two Al vacancies), while NiAl displays vacancy annihilation (the converse case, where an Al atom goes onto a constitutional Ni vacancy and the ensuing Al vacancy annihilates with another constitutional Ni vacancy, shrinking the crystal by one unit cell).

A.4 Order and disorder

In general, the state of lowest energy for a system in a given composition is an ordered state: for short-range interactions, some local motifs are energetically favoured, and building a structure by fitting such building blocks together leads to a regular arrangement. In most cases, this will lead to translational symmetry.[6] In elemental systems, the only intrinsic defects apart from phonons are vacancies and interstitials, both of which have quite high formation energies, so that the system does not display much disorder up to the melting point. In contrast, in multi-component systems where the constituent elements are not too different from the chemical point of view, often significant disorder in the crystalline state can appear at elevated temperatures, affecting the properties of materials significantly. Specifically, the assignment of specific elements to specific sublattices in an ordered compound will be disturbed, and at higher temperature it can transform into a disordered state of higher symmetry (where sublattices lose their distinction), but where the interactions between the species still lead to correlations between the occupations of neighbouring sites. These two aspects, i.e. the degree to which a given sublattice is occupied by a single element, and on the other hand correlations between neighbouring sites in a disordered system, go under the terms long-range and short-range order, and will be discussed here. Note that, as was already related in the previous section, non-ideal occupations of sites also lead to displacements of the atoms from the ideal lattice.

A.4.1 Long-range order

Consider a binary system that displays B2 order (or any ordered structure with two inequivalent sites per unit cell). The degree of long-range order is quantified by the long-range order parameter, which is often denoted η or S. In general it is defined in terms of the compositions on the respective sublattices such that it is equal to zero for the disordered case (where the two sublattices have equal elemental make-up). An appropriate definition for the case at hand would be

$$\eta = c_\alpha^A - c_\beta^A, \tag{A.4.1}$$

that is the difference of the concentration of species A on the two sublattices. The highest possible degree of order for a given composition is when one sublattice is occupied exclusively by one element, corresponding to

$$\eta_{\max} = 1 - |2c^A - 1|. \tag{A.4.2}$$

Note that the role of element A is not special, swapping A with B and α with β would give an equivalent definition. Conversely, the concentrations on the sublattices follow as

$$c_\alpha^A = c^A + \eta/2 \qquad \text{and} \qquad c_\beta^A = c^A - \eta/2. \tag{A.4.3}$$

---

[6]Exceptions to this rule are charge- or spin-density wave states, which result from non-local interactions, and quasicrystals, which result from local rotational symmetries that are incompatible with translational symmetry.

On the other hand, for the $L1_2$ structure with one α site per unit cell and three equivalent sites β_i, a long-range order parameter can be defined formally identical as in the B2 case

$$\eta = c_\alpha^A - c_\beta^A, \tag{A.4.4}$$

but here the sublattice concentrations are now given by

$$c_\alpha^A = c^A + 3/4\eta \qquad \text{and} \qquad c_\beta^A = c^A - 1/4\eta. \tag{A.4.5}$$

In the $L1_2$ the three β sublattices are equivalent, therefore $c_{\beta_i}^X =: c_\beta^X$. The highest possible degree of order is given by

$$\eta_{\max} = \frac{2}{3}\left(1 + 2c^A - |4c^A - 1|\right). \tag{A.4.6}$$

More complicated ordered structures accordingly are described by more complicated long-range order parameters. Take for example the $L2_1$ Heusler structure with nominal composition ABC_2 and four sublattices α, β, γ_1 and γ_2, where the last two are equivalent. An intuitive choice would be to first define an order parameter describing the B2-type order, i.e. to which extent the C atoms stay on the γ_i sublattices

$$\eta_{B2} = c_\gamma^C - \left(c_\alpha^C + c_\beta^C\right)/2 \tag{A.4.7}$$

and an $L2_1$-type order parameter describing the division of A and B onto α and β

$$\eta_{L2_1} = \left(c_\alpha^A + c_\beta^B - c_\alpha^B - c_\beta^A\right)/2, \tag{A.4.8}$$

and finally whether C goes rather onto α or β

$$\eta' = c_\alpha^C - c_\beta^C. \tag{A.4.9}$$

Note that the purpose of long-range parameters is to give a description of the elemental make-up on the sublattices that is non-redundant and as symmetrical as possible. Indeed, one could also use the sublattice concentrations themselves, however, for instance in the $L2_1$-case these are nine variables (three elements on three inequivalent sites) that are subject to six linear equations (three for constraining the overall concentrations and three for summing the occupation of each lattice to one). Note further that in systems where off-stoichiometry is accommodated by constitutional vacancies, the constraint for the sublattice occupations to sum to one would not hold any more. In this case, it is more appropriate to consider vacancies as an additional species.

Finally, attention has to be drawn to the fact that in physical reality, a superstructure nucleates at different locations in the sample, leading to so-called *anti-phase domains*, at the boundaries of which the assignment of sublattices jumps (analogously to polycrystal grains). Further, in the case of a dislocation, a global assignment of sites to sublattices is even not possible any more. This demonstrates that one has to understand the sublattice compositions in a local sense for above description to be meaningful, as otherwise the presence of anti-phase domains would average out the differences in the sublattice compositions.

A.4.2 Short-range order

In general, at temperatures where a given multi-component system has lost its long-range order, it will still display short-range order. This means that not all possibilities of occupying the lattice sites with the distinct elements are equally probable, rather some local configurations are favoured by free energy and therefore more frequent.

Such local correlations on the pair level are quantified by the Warren-Cowley short-range order parameters. Consider a binary system with composition c (i.e. the concentration of element A is c and the concentration of element B is $1 - c$) on a Bravais lattice. For a given lattice vector $\vec{x}$ let $P_{\vec{x}}^{A,B}$ be the probability for site $\vec{y}$ to be occupied by A and site $\vec{y} + \vec{x}$ by B, averaged over all $\vec{y}$ (i.e. it is half the probability for a pair of sites related by a vector $\vec{x}$ to be occupied by distinct elements). The short-range order parameters are then given by

$$\alpha_{\vec{x}} = 1 - \frac{P_{\vec{x}}^{A,B}}{c(1 - c)}. \tag{A.4.10}$$

Note that in the absence of correlations (that is for very high temperature or large $\vec{x}$) $P_{\vec{x}}^{A,B} = c(1 - c)$, therefore $\alpha_{\vec{x}} = 0$ in this case. Negative values of $\alpha_{\vec{x}}$ correspond to negative correlations, that is preferred unlike pairs, while positive values correspond to like pairs. In the extreme case where an atom A at $\vec{y}$ implies also an atom A at $\vec{y} + \vec{x}$ (equivalently for B), $\alpha_{\vec{x}}$ equals one (which is trivially fulfilled for $\vec{x} = 0$).

Short-range correlations are present also for long-range ordered systems that have some degree of disorder. For instance in a B2 system with antisites on both sublattices, it is conceivable that the β neighbours of an α antisite have an increased probability to host antisites themselves. It is possible to use the definition (A.4.10) directly for superstructures. In this case, the parameters $\alpha_{\vec{x}}$ will not decay to zero with large $\vec{x}$, rather they will alternate between positive and negative values defined by the long-range order parameters. A more sophisticated generalization of (A.4.10) is to consider three sets of $\alpha_{\vec{x}}$: one with vectors linking sites on the α sublattice, another for sites on the β sublattice, and a third for vectors between the sublattices. Using the appropriate sublattice concentrations in the denominator will lead to a qualitative similar behaviour as in the disordered case, i.e. a decay towards zero for large $\vec{x}$.

A.5 Statistical mechanics and thermodynamics of point defects and order

At zero temperature, a sample would in principle assume the state of lowest internal energy that is compatible with the conditions imposed on it (such as particle number or volume). At non-zero temperature, it tends to minimize its free energy, however (which coincides with the internal energy at $T = 0$). This implies the consideration of ensembles of microstates, i.e., statistical mechanics, which will be treated in the following. Specifically, approximate expressions for

free energies in different models will be derived, which will be used in A.6 to derive phase diagrams. Note that, indeed, ambient temperature would be low enough compared to typical excitations energies for being able to approximate the thermodynamic ground-state by the zero-temperature ground-state for many materials properties. However, in most cases samples are not in equilibrium at ambient temperatures with regard to properties such as order, as the slowing kinetics during cooling freeze the state of the sample at some higher temperature.

The setting for most of this section will be the canonical ensemble. As we consider a classical system of interacting particles (i.e., we do not consider electrons explicitly), the degrees of freedom are the positions of the atoms, where atoms of same species are indistinguishable. More specifically, we will separate configurational and vibrational degrees of freedom. The latter give rise to vibrational entropies, which we consider as fixed, so that the microstate of the system is actually described by specifying the occupation of the lattice sites.

In the canonical ensemble, the weight of a given microstate σ is proportional to the Boltzmann factor which depends on the energy according to

$$p(\sigma) \propto \exp\bigl(-E(\sigma)/k_\mathrm{B}T\bigr). \tag{A.5.1}$$

In a description by macroscopic parameters (e.g., order) denoted by ψ, the probability for the system to have a given value of ψ follows as

$$p(\psi) \propto W(\psi)\exp\bigl(-E(\psi)/k_\mathrm{B}T\bigr), \tag{A.5.2}$$

where $W(\psi)$ is — sloppily speaking — the number of compatible microstates, and $E(\psi)$ is the internal energy, averaged over these microstates. The grand-canonical ensemble is analogous, but with the additional freedom of non-conserved particle numbers. Here, the internal energies are formally modified by a term linear in the number of particles, with the chemical potential μ as the proportionality constant (for multi-component systems each species has a distinct chemical potential).

On the other hand, in the thermodynamic description the equilibrium state of a system is where its free energy is minimized with respect to ψ. The free energy is defined as

$$F(\psi) = U(\psi) - TS(\psi), \tag{A.5.3}$$

with U the internal energy[7] and S the entropy. The connection to statistical mechanics is made by equating

$$S(\psi) = k_\mathrm{B}\log\bigl(W(\psi)\bigr). \tag{A.5.4}$$

Indeed, for fixed temperature minimizing $F(\psi)$ is equivalent to maximizing

$$\exp\bigl(-F(\psi)/k_\mathrm{B}T\bigr) = W(\psi)\exp\bigl(-U(\psi)/k_\mathrm{B}T\bigr), \tag{A.5.5}$$

which shows that the thermodynamic viewpoint is equivalent to replacing the distribution of ψ according to equation (A.5.2) by the ψ at its peak, which is justified in the limit of large particle numbers.

---

[7]The internal energy is commonly denoted by U if it is understood in a thermodynamical setting, and by E if it is the energy corresponding to some specific (micro)state.

A.5.1 Isolated point defects

We first treat elemental systems, with vacancies as the kind of considered point defect. The number of ways to arrange N atoms and M vacancies on a lattice is

$$W(M) = \frac{(N+M)!}{N!M!}, \tag{A.5.6}$$

therefore by invoking the Stirling approximation the associated configurational entropy per lattice site is

$$\begin{aligned} S^{\mathrm{conf}}(c) &= \frac{1}{N+M} k_{\mathrm{B}} \log\big(W(M)\big) \\ &= \frac{1}{N+M} k_{\mathrm{B}} \big((N+M)\log(N+M) - N\log(N) - M\log(M)\big) \\ &= -k_{\mathrm{B}}\big(c\log(c) + (1-c)\log(1-c)\big) \end{aligned} \tag{A.5.7}$$

with $c = M/(N+M)$. The free energy per lattice site is

$$F(c) = cE^{\mathrm{f}} - T\big(S^{\mathrm{conf}}(c) + cS^{\mathrm{f}}\big), \tag{A.5.8}$$

where E^{f} and S^{f} are the formation energy and entropy, respectively. Setting the derivative with respect to c to zero

$$0 = E^{\mathrm{f}} + T\Big(k_{\mathrm{B}}\log\big(c/(1-c)\big) - S^{\mathrm{f}}\Big) \tag{A.5.9}$$

gives

$$\frac{c}{1-c} = \exp\big(-E^{\mathrm{f}}/k_{\mathrm{B}}T + S^{\mathrm{f}}/k_{\mathrm{B}}\big). \tag{A.5.10}$$

On the other hand, considering a fixed number of lattice sites at a varying number of atoms (i.e., a grand-canonical ensemble) gives directly a probability for a given site to be occupied by a vacancy and thereby a vacancy concentration of

$$c = \frac{\exp\big(-E^{\mathrm{f}}/k_{\mathrm{B}}T + S^{\mathrm{f}}/k_{\mathrm{B}}\big)}{1 + \exp\big(-E^{\mathrm{f}}/k_{\mathrm{B}}T + S^{\mathrm{f}}/k_{\mathrm{B}}\big)} = \frac{1}{1 + \exp\big(E^{\mathrm{f}}/k_{\mathrm{B}}T - S^{\mathrm{f}}/k_{\mathrm{B}}\big)}, \tag{A.5.11}$$

which can be immediately shown to be consistent with above equation.

For small concentrations, the free energy is therefore minimized at a vacancy concentration of

$$c = \exp\big(-E^{\mathrm{f}}/k_{\mathrm{B}}T + S^{\mathrm{f}}/k_{\mathrm{B}}\big) = c_0 \exp\big(-E^{\mathrm{f}}/k_{\mathrm{B}}T\big). \tag{A.5.12}$$

Treating interstitials, the other kind of intrinsic point defect in elemental systems, in the canonical ensemble would lead to a slightly different picture, as here introducing a defect reduces instead of enlarges the number of lattice sites. Still, for small c, which is in any case implied by considering point defects in isolation, an equation of the form of (A.5.12) is appropriate.

For ordered compounds, the situation becomes more complicated, as already discussed in A.3.5. Here the grand-canonical setting with fixed number of lattice

sites is most convenient. In the simplest case of a binary compound with two sublattices, with vacancies and antisites on both sublattices as considered point defects, for instance the concentration of vacancies on the α-sublattice is given by

$$c_\alpha^{\mathrm{v}} = \frac{\exp\left(-(E_\alpha^{\mathrm{v}} - \mu)/k_{\mathrm{B}}T + S_\alpha^{\mathrm{v}}/k_{\mathrm{B}}\right)}{1 + \exp\left(-(E_\alpha^{\mathrm{v}} - \mu)/k_{\mathrm{B}}T + S_\alpha^{\mathrm{v}}/k_{\mathrm{B}}\right) + \exp\left(-(E_\alpha^{\mathrm{B}} - 2\mu)/k_{\mathrm{B}}T + S_\alpha^{\mathrm{B}}/k_{\mathrm{B}}\right)}. \quad \text{(A.5.13)}$$

In order to describe an experimental situation of fixed elemental composition, μ has to be chosen for each T so that the overall composition resulting from the concentrations of the species on the sublattices is correct. Considering the low-temperature limit of above formula, it can be seen that the behaviour as reported already in A.3.5 results: With decreasing temperature also subtle energy differences become amplified in the Boltzmann factors, so that at some point practically only one constitutional defect remains that guarantees the off-stoichiometry. The concentration of this defect has then to be independent of temperature, therefore its effective formation energy (the numerator in the exponent of the Boltzmann factor) has to be equal to zero, thereby specifying μ.

Finally, a word of caution is in order: The theoretical prediction of an *Arrhenius behaviour* as evidenced by Eq. (A.5.12) has often been taken as a theoretical necessity for the concentration of defect species, and deviations from it have been interpreted as being due to multiple defect species at comparable concentrations (e.g., vacancy concentrations below the melting point in excess of the Arrhenius prediction have been construed as indications of divacancies). Apart from being restricted to the elemental case, this also rests on the assumption of the defect's formation entropy being constant. In fact, recent calculations of defect concentrations have demonstrated that anharmonic vibrational effects can explain the deviations from Arrhenius behaviour for prototypical systems, ruling out divacancies at measureable concentrations.

A.5.2   Models for the internal energy

The most general expression for the internal energy of a microstate assuming short-range interactions and translation symmetry is

$$E(\sigma) = \sum_{\vec{x}} V_{\sigma(\vec{x}+\vec{s}_0),\dots,\sigma(\vec{x}+\vec{s}_N)}, \quad \text{(A.5.14)}$$

where $\sigma(\vec{x})$ is the occupation function, i.e., $\sigma(\vec{x}) = 0$ means that site $\vec{x}$ is occupied by element 0 and so on, and $V_{i_0,\dots,i_N}$ are the energies of local clusters, where for instance $V_{0,\dots}$ is the energy contribution by a cluster centred around $\vec{x}$ that has the site at position $\vec{s}_0$ occupied by 0 and so on.

However, in statistical modelling one commonly considers only pair-wise interactions. The reason is that correlations (if they are treated at all, see below) are also only treated on the pair level. The corresponding specialization of above expression is

$$E(\sigma) = \sum_{\vec{x}} \sum_{\vec{s}} V^{\vec{s}}_{\sigma(\vec{x}),\sigma(\vec{x}+\vec{s})}, \quad \text{(A.5.15)}$$

where $\vec{s}$ covers all pairs within the interaction range.

For the case of a binary system, a further specialization is convenient. The internal energy per lattice site is

$$
\begin{aligned}
E(\sigma) &= \frac{1}{N} \sum_{\vec{x}} \sum_{\vec{s}} V^{\vec{s}}_{\sigma(\vec{x}),\sigma(\vec{x}+\vec{s})} \\
&= \sum_{\vec{s}} \left(P^{A,A}_{\vec{s}} V^{\vec{s}}_{A,A} + 2 P^{A,B}_{\vec{s}} V^{\vec{s}}_{A,B} + P^{B,B}_{\vec{s}} V^{\vec{s}}_{B,B} \right) \\
&= \sum_{\vec{s}} \left((c - P^{A,B}_{\vec{s}}) V^{\vec{s}}_{A,A} + 2 P^{A,B}_{\vec{s}} V^{\vec{s}}_{A,B} + (1 - c - P^{A,B}_{\vec{s}}) V^{\vec{s}}_{B,B} \right) \\
&= V_0 + c V_1 + \sum_{\vec{s}} P^{A,B}_{\vec{s}} V(\vec{s}),
\end{aligned}
\tag{A.5.16}
$$

where N is the number of lattice sites, c the concentration of element A, and

$$
V_0 = \sum_{\vec{s}} V^{\vec{s}}_{B,B}
\tag{A.5.17a}
$$

$$
V_1 = \sum_{\vec{s}} \left(V^{\vec{s}}_{A,A} - V^{\vec{s}}_{B,B} \right)
\tag{A.5.17b}
$$

$$
V(\vec{s}) = 2 V^{\vec{s}}_{A,B} - V^{\vec{s}}_{A,A} - V^{\vec{s}}_{B,B}.
\tag{A.5.17c}
$$

With the Warren-Cowley short-range order parameters this can be expressed as

$$
E = V_0 + c V_1 + c(1-c) \sum_{\vec{s}} V(\vec{s})(1 - \alpha_{\vec{s}}).
\tag{A.5.18}
$$

A.5.3 The Bragg-Williams approximation

The Bragg-Williams approximation is the simplest model for the free energy of general multi-component systems. It is a mean-field method, which means that it does not consider local correlations at all, it assumes any atom to feel only an average environment. It can therefore only treat long-range ordering phenomena.

A.5.3.1 Case: Disordered systems on a Bravais lattice

In its simplest form it is a model for the free energy of a disordered binary system, which is called *solid solution*. Neglecting correlations, the entropy depends only on c according to the expression (A.5.7) already derived for isolated point defects, and the internal energy per lattice site is (Eq. (A.5.18) with $\alpha_{\vec{s}} = 0$)

$$
E = V_0 + c V_1 + c(1-c) \sum_{\vec{s}} V(\vec{s}),
\tag{A.5.19}
$$

giving a free energy per lattice site of

$$
F(T,c) = V_0 + c V_1 + c(1-c) \sum_{\vec{s}} V(\vec{s}) - T S^{\text{conf}}(c).
\tag{A.5.20}
$$

The model corresponding to this expression is called the *regular solution*. If there is no enthalphy of mixing (no energy terms apart from a constant term and a term linear in composition), the free energy is determined only by entropy (and Eq. (A.5.7) is exact), in which case it would be called *ideal solution*.

A.5.3.2   Case: Superstructure with two sites per unit cell

Here we consider the simplest kind of superstructure on a Bravais lattice, having two sublattices with different compositions (for instance, the B2 or $L1_0$ structures). Specifically, let c_α and c_β be the concentrations of one element on the respective sublattices. The entropies of the sublattices are additive, only with the interaction care has to be taken with respect to the compositions at the participating sites. The appropriate expression for the free energy per unit cell is

$$
\begin{aligned}
F(T, c_i) = {}& 2V_0 + (c_\alpha + c_\beta)V_1 + \big(c_\alpha(1 - c_\alpha) + c_\beta(1 - c_\beta)\big)\sum_{\vec{s}} V(\vec{s}) \\
& + (c_\alpha + c_\beta - 2c_\alpha c_\beta)\sum_{\vec{t}} V(\vec{t}) - T\big(S^{\mathrm{conf}}(c_\alpha) + S^{\mathrm{conf}}(c_\beta)\big),
\end{aligned}
\tag{A.5.21}
$$

where $\vec{s} \in \{\langle 100\rangle, \langle 110\rangle, \langle 111\rangle, \dots\}$ in the B2 case connects sites on the same sublattice, and $\vec{t} \in \{1/2\langle 111\rangle, 1/2\langle 311\rangle, \dots\}$ connects sites on different sublattices.

A.5.3.3   Case: $L1_2$ superstructure

In the $L1_2$-structure, the underlying fcc lattice decomposes into four sublattices, three of which have the same composition c_α and a fourth has a potentially different composition c_β. The free energy is now given by

$$
\begin{aligned}
F(T, c_i) = {}& 4V_0 + (3c_\alpha + c_\beta)V_1 + \big(3c_\alpha(1 - c_\alpha) + c_\beta(1 - c_\beta)\big)\sum_{\vec{s}} V(\vec{s}) \\
& + \big(3c_\alpha + c_\beta - 2c_\alpha(c_\alpha + c_\beta)\big)\sum_{\vec{t}} V(\vec{t}) - T\big(3S^{\mathrm{conf}}(c_\alpha) + S^{\mathrm{conf}}(c_\beta)\big), \quad \text{(A.5.22)}
\end{aligned}
$$

where again $\vec{s} \in \{\langle 100\rangle, \langle 110\rangle, \langle 111\rangle, \dots\}$ are the vectors linking sites on the fourth sublattice and $\vec{t} \in \{1/2\langle 110\rangle, 1/2\langle 211\rangle, 1/2\langle 310\rangle, \dots\}$ all others.

A.5.4   The cluster variation method

The cluster variation method is a consistent way of expanding local configurations in terms of correlation variables up to some order and computing the corresponding configurational free energies.

Consider for instance the fcc lattice. The natural choices for the clusters are

- the one-point cluster consisting of a single site

- the two-point cluster consisting of a nearest-neighbour pair of sites

- the three-point cluster, an equilateral triangle harbouring three two-point cluster

- the four-point cluster, a regular tetrahedron with four three-point cluster as faces.

In those clusters all sites are equivalent with respect to the cluster, but note that for higher-order clusters this is not the case any more. Note also that for larger clusters two-point clusters that are not nearest-neighbour pairs appear.

The variables that describe the configuration of a system are $x_0 = p_A$ and $x_1 = p_B$, giving the probability for one-point clusters to consist of zero or one A-atom, respectively, $y_0 = p_{A,A}$, $y_1 = p_{A,B} = p_{B,A}$ and $y_2 = p_{B,B}$ for the two-point clusters, z_i and w_i defined analogously for the three- and four-point clusters, respectively. Note that the degrees of freedom spanned by these variables are quite small: First, the cluster probabilities on a given order have to sum to 1, for instance $\sum_i \binom{4}{i} w_i = 1$. Further, the cluster probabilities on a given order completely specify those of the previous order (and by induction of all smaller orders), for instance $x_0 = y_0 + y_1$. This would allow to define one scalar cluster correlation variable per order up to the tetrahedron level according to $\xi_1 = x_1 - x_0$, $\xi_2 = y_2 - 2y_1 + y_0$ and so on.

Given either the correlation variables ξ_i or the cluster probabilities for some order, it is easy to compute the internal energy. For instance, in the commonly used pair-interaction approximation the two-point cluster probabilities y_i can directly be used with Eq. (A.5.16). In contrast, computing the entropy is much harder in the presence of correlations and exact expressions are known only for very special cases. This is where the cluster variation method shows a way of obtaining increasingly accurate approximations.

The linear chain in the pair-level approximation shall demonstrate the concepts as easiest conceivable example: Consider an ensemble of L systems with some specific choice for the cluster probabilities. Assume that you construct the configurations starting from one end, and that at some given stage during this construction all sites up to site j have been assigned, and the resulting clusters conform to the chosen probabilities. We will now compute the number of possibilities there are in assigning an occupation to site $j + 1$ so that the newly resulting clusters also fulfill the probabilities. In the ensemble there are $x_0 L$ systems where site j is occupied by A, and to get the correct probabilities for AA clusters there have to be $y_0 L$ systems among those $x_0 L$ systems where site $j + 1$ is also occupied by A, and the remaining $y_1 L$ systems have to have B on $j + 1$. For the $x_1 L$ systems with B at j the situation is analogous. Specifically, the number of microstates in the ensemble increases by a factor of

$$G_L = \binom{x_0 L}{y_0 L}\binom{x_1 L}{y_2 L} = \frac{\prod_i (x_i L)!}{\prod_j \left((y_j L)!\right)^{n_{y_j}}}, \tag{A.5.23}$$

where n_{y_j} is the multiplicity of a cluster (in the specific example for pairs there are AB and BA clusters, therefore $n_{y_1} = 2$). Defining the abbreviations

$$\{\}_L = L! \tag{A.5.24a}$$

$$\{\text{Point}\}_L = \prod_i (x_i L)! \tag{A.5.24b}$$

$$\{\text{Pair}\}_L = \prod_j \left((y_j L)!\right)^{n_{y_j}} \tag{A.5.24c}$$

and so on, we can write

$$G_L = \frac{\{\text{Point}\}_L}{\{\text{Pair}\}_L}. \tag{A.5.25}$$
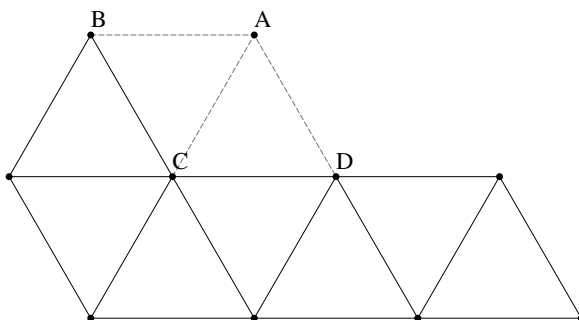
Figure A.1: Inserting an atom in the two-dimensional hexagonal lattice in *Halb-kristalllage*.

Specifically, the entropy per lattice site and system is

$$S/k_\mathrm{B} = \frac{\log(G_L)}{L} = \sum_i x_i \log x_i - \sum_j n_{y_j} y_j \log y_j. \tag{A.5.26}$$

In a description on the level of point correlations the result would be

$$G_L = \frac{\{\}_L}{\{\text{Point}\}_L}, \tag{A.5.27}$$

corresponding to an entropy per lattice site of

$$S/k_\mathrm{B} = \frac{\log(G_L)}{L} = -\sum_i x_i \log x_i. \tag{A.5.28}$$

Indeed, the point-level cluster description (i.e., only as a function of densities) is nothing else than the Bragg-Williams approach, reproducing the entropy expression (A.5.7) derived there. Note also that evaluating Eq. (A.5.26) with pair-level probabilities y_i as uncorrelated products of point-level probabilities

$$y_0 = x_0^2 \tag{A.5.29a}$$

$$y_1 = x_0 x_1 \tag{A.5.29b}$$

$$y_2 = x_1^2 \tag{A.5.29c}$$

reduces to the point-level description of Eq. (A.5.28).

For the special case of a linear chain with only nearest-neighbour interactions the cluster variation description is exact already at the pair level. For higher-dimensional lattices a description by finite clusters is only an approximation, however. Next we will consider the pair-level description of general Bravais lattices, with the case of a two-dimensional hexagonal lattice illustrated in Fig. A.1 as an example.

We consider the number of possibilities to insert an atom in *Halbkristalllage* at site A. As in the case of the linear chain, we have

$$G_L' = \frac{\{\text{Point}\}_L}{\{\text{Pair}\}_L} \tag{A.5.30}$$

possibilities for doing so with respect to neighbouring site B. Now the occupation probability of A is correct on the point-level (and also the A-B pair is correct on the pair level). To have a correct probability also for the A-C pair, a similar factor is necessary. However, now site A is considered doubly. To correct for this fact, we divide by the contribution due to site A on the point level, i.e. multiply by the correction factor

$$K = \frac{\{\text{Point}\}_L}{\{\,\}_L} \tag{A.5.31}$$

as already used above. Concludingly, for a lattice with a coordination number of Z (i.e. $Z/2$ additional bonds per inserted atom in *Halbkristalllage*) we have

$$G_L = \frac{\{\text{Point}\}_L^{Z-1}}{\{\text{Pair}\}_L^{Z/2}\{\,\}_L^{Z/2-1}}, \tag{A.5.32}$$

and an entropy per lattice site of

$$S/k_{\text{B}} = \frac{\log(G_L)}{L} = (Z-1)\sum_i x_i \log x_i - Z/2\sum_j n_{y_j} y_j \log y_j \tag{A.5.33}$$

for lattices of arbitrary dimension.

Finally, as a more complicated example we treat the two-dimensional hexagonal lattice in the triangle-approximation. Here we have a factor of

$$G_L' = \frac{\{\text{Pair}\}_L}{\{\text{Triangle}\}_L} \tag{A.5.34}$$

with respect to the A-B-C triangle. The A-C-D triangle gives a similar factor, while the double counting of the A-C pair necessitates a correction factor of

$$K = \frac{\{\text{Pair}\}_L}{\{\text{Point}\}_L} \tag{A.5.35}$$

giving

$$G_L = \frac{\{\text{Pair}\}_L^3}{\{\text{Triangle}\}_L^2\{\text{Point}\}_L}, \tag{A.5.36}$$

and an entropy per lattice site of

$$S/k_{\text{B}} = \frac{\log(G_L)}{L} = -\sum_i x_i \log x_i + 3\sum_j n_{y_j} y_j \log y_j - 2\sum_k n_{z_k} z_k \log z_k. \tag{A.5.37}$$

A.5.5 Short-range order in the high-temperature limit

Here the cluster variation method shall be applied to derive a quantitative expression for short-range order. Consider a binary system on a Bravais lattice, initially only with pair interactions between nearest neighbours that would lead to ordering at low temperatures (that is, $V(\vec{s})$ in the nomenclature of Sect. A.5.2 shall be negative and will in the following be denoted as V_2).
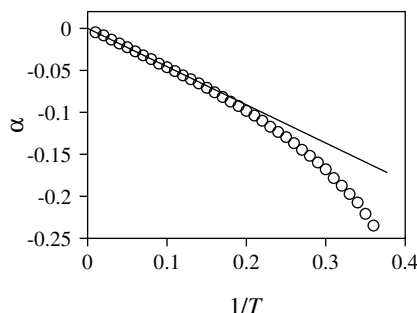
Figure A.2: The nearest-neighbour Warren-Cowley short-range order coefficient as function of inverse temperature for a solid solution on the bcc lattice at composition $c = 0.35$. Temperature is measured in units of $-V_2$, the ordering transition is around $T = 2.65$ in these units. Points are due to Monte Carlo-simulation, the line corresponds to expression (A.5.41).

In the pair approximation of the cluster variation method, the expression for the free energy reads

$$F(T, c, p^{AB}) = V_0 + cV_1 + Zp^{AB}V_2 - k_B T\Big((Z-1)\big(c\log c + (1-c)\log(1-c)\big)$$
$$- \tfrac{Z}{2}(p^{AA}\log p^{AA} + 2p^{AB}\log p^{AB} + p^{BB}\log p^{BB})\Big), \quad \text{(A.5.38)}$$

where p^{AB}, p^{AA} and p^{BB} denotes the nearest-neighbour pair probabilities, with the latter two following from the first.

For fixed composition, the system will minimize its free energy with respect to the pair probabilities, thus

$$0 \stackrel{!}{=} \frac{\partial F}{\partial p^{AB}} = ZV_2 + k_B TZ/2\big(-1 - \log p^{AA} + 2 + 2\log p^{AB} - 1 - \log p^{BB}\big) \quad \text{(A.5.39)}$$

which is equivalent to

$$\exp(-2V_2/k_B T) = \frac{p^{AB}p^{AB}}{p^{AA}p^{BB}}. \tag{A.5.40}$$

At large temperatures correlations will be small. Expanding above expression to first order in $1/k_B T$ and Warren-Cowley parameter α leads to the result

$$\alpha = \frac{2V_2}{k_B T}c(1-c). \tag{A.5.41}$$

Fig. A.2 shows that in a typical situation this expression is quite accurate for temperatures above about two times the ordering temperature.

In the presence of pair interactions beyond nearest neighbours, both the energy as well as the entropy in the pair level approximation of the cluster variation method are essentially additive with respect to the different kinds of pairs. Thus, taking the derivatives would lead to decoupled equations, so that in the high-temperature limit it is only the direct interaction between sites that determines

the corresponding pair probabilities. Indirect interactions, where the occupation of a given site $\vec{x}$ influences some site $\vec{y}$, which in turn affects a site $\vec{z}$, while there are no direct energetical interactions between $\vec{x}$ and $\vec{z}$, scale according to the derivation given above at least with $1/T^2$.

A.6 Phases and phase diagrams

A.6.1 Thermodynamic phases and phase transitions

A *thermodynamic phase* corresponds to a region in macroscopic phase space inside of which the equilibrium value of any property varies smoothly. These regions are separated by phase boundaries, which are the locations in phase space where there is a property that varies non-smoothly. These phase boundaries, which in the first line are abstract entities in phase space, can often also be observed as spatial features in physical systems, such as the solid-liquid interface of ice in water or the liquid-liquid interface in an oil-water mixture.

There is a multitude of ways phases can differ. A very fundamental difference is in the state of matter, e.g., solid, liquid, or gaseous, and in addition more exotic states such as a Bose-Einstein condensate. With respect to materials physics, we will consider primarily solid phases. The principal external degrees of freedom here are temperature and the composition of a multi-component system, while around ambient conditions the effect of pressure can often be neglected for solids. The reaction of the system to changes in these external parameters, that is the internal parameters that display the non-smooth behaviour, can for instance pertain to magnetism (from paramagnetic to ferro- or antiferromagnetic, or between ordered magnetic phases), any kind of structural transition (involving the exchange of atoms such as in disorder-order transitions or only small-scale displacements in displacive transitions), or non-continuous changes in compositions.

A main distinction of phase transitions is whether there is a latent heat or not, corresponding in the classification due to Paul Ehrenfest to first-order transitions (where the first derivative of the free energy shows a discontinuity) and higher-order transitions (discontinuity in a higher derivative), respectively. Examples for first-order transitions are discontinuous transitions such as melting, while magnetic transitions are typically of second order. Interestingly, we will see that already among the simplest order-disorder transitions there are examples for either kind.

A further important aspect of phase transitions is whether there is a symmetry breaking involved. For instance, in the melting transition the discrete translational symmetry of the crystalline solid is broken, while in the liquid-vapour transition there is no further symmetry to be broken. Also in paramagnetic/ (anti-)ferromagnetic transitions and disorder-order transitions a symmetry is reduced, as the fundamental lattice in the parent phase decays into inequivalent sublattices.

A *metastable phase* is a phase that is actually not the ground-state phase, but

which can exist when the kinetics that would bring the system to equilibrium become longer than experimental timescales at low temperature. Relevant examples of metastable phases are the diamond modification of carbon (where graphite would be the ground state at ambient pressure) and Fe_3C (cementite) in the iron-carbon system, where only the pure elements (i.e., iron and graphite) are actually ground-state phases. Glasses show a complicated situation: while the amorphous solid is always only metastable, it is not clear whether it is only an extension of the liquid phase to lower temperatures or whether there is some well-defined liquid-glass transition affecting primarily the dynamics of the system.

A final subtlety has to be noted: For instance, in the temperature-pressure phase diagram of an elemental system the liquid-vapour phase boundary ends at a critical point, above which there is no point to distinguish the liquid and vapour phase. According to above definition, they are therefore the same phase, as they share a single common region in phase space (in fact, they do have the same symmetry, as mentioned already). However, at low temperature and low pressure the two phases are clearly distinct, and commonly they are considered as different phases. Also in binary solid-state systems that are miscible at high temperatures but have a low-temperature miscibility gap, the A- and B-rich phases have to be considered as distinct at low temperatures, while they are connected at high temperatures.

A.6.2   Convexity, bitangents and the lever rule

A system that is held at some fixed temperature will minimize its free energy. Here we will only consider the resulting thermodynamic ground state given the external parameters, which effectively are the composition of the system and temperature. We will not consider the way this ground state is reached from a given initial state, which is the question of kinetics.

In principle, the degrees of freedom can be classified into three categories: first, there are qualitative distinctions corresponding to different phases, such as liquid, bcc, fcc or so on. Further, there are continuous degrees of freedom such as parameters describing the unit cell dimensions, positions of sublattices, and their elemental make-up. As we normally consider a case of fixed (and low) pressure, all these internal parameters are not fixed by external parameters and will be minimized.

The composition makes up the third category. It is a continuous degree of freedom, but in contrast to those of the second category it is constrained by particle number conservation. However, this does not forbid spatial composition inhomogeneities, where the local compositions deviate from the mean value.

Consequently, the thermodynamic ground state of a multi-component system results in the following way: Consider a system of J components and specific values for the external parameters (such as temperature). Consider a number of qualitatively different phases the system can display, and assume that their specific free energies are given by $F_i(c_j, \beta_l^i)$, where i enumerates the phases, β_l^i are the respective internal parameters, and c_j are the concentrations of the respective

elements. Define

$$F_i'(c_j) = \min_{\beta_l^i} F_i(c_j, \beta_l^i) \tag{A.6.1}$$

and

$$F'(c_j) = \min_i F_i'(c_j), \tag{A.6.2}$$

that is to say $F_i'(c_j)$ is the resulting free energy of phase i at composition c_j with optimal choice of the internal parameters, and $F'(c_j)$ is the absolute minimum free energy the system can have at this composition (with optimal choice of the qualitative phase).

What remains now is the freedom of concentration inhomogeneities: For this end, assume that the system decays into K regions with concentrations c_j^k and weight x^k. Of course we have

$$\sum_k x^k = 1 \tag{A.6.3}$$

and

$$\sum_k x^k c_j^k = c_j', \tag{A.6.4}$$

where c_j' is the overall composition.

Free energy is additive, meaning that if a system is composed of a number of subsystems, the total free energy of the system is the sum of the subsystems' free energies. Consequently, the free energy of an inhomogeneous system is given by

$$F = \sum_k x^k F'(c_j^k), \tag{A.6.5}$$

which can potentially be lower than $F'(\sum_k x^k c_j^k)$.

Note that this issue corresponds to a question of *convexity*: If F' is not convex, there are compositions where the system can gain free energy by a phase separation, i.e., separating into regions with respective weights x^k and compositions c_j^k, so that the weighted average free energy is lower than the free energy of the homogeneous system would be. Allowing for phase separation, the free energy is yet again reduced to the lower convex envelope of F': Discussing from here on only the binary case for simplicity, this corresponds to finding all lower bitangents and replacing the F' in the region between the tangent points by the bitangent.

Physically, a system with a total composition c that falls within the range of such a bitangent is in a two-phase state: let c^1 and c^2 be the compositions in the tangent points, then the system decomposes into a phase with composition c_1 and weight $x_1 = (c_2 - c)/(c_2 - c_1)$ and a phase with composition c_2 and weight $x_2 = (c - c_1)/(c_2 - c_1)$. This relation is termed the *lever rule* in analogy to the case of mechanics, with x_i as the forces, c_i as their points of attack, and c as the pivot. Specifically, note that the compositions of the two phases do not depend on the total composition.
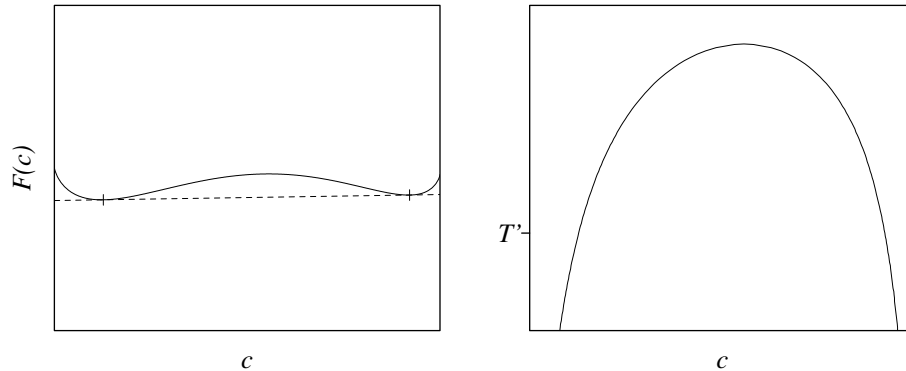
Figure A.3: Miscibility gap: free energy for representative temperature T' where demixing occurs (left), resulting phase diagram (right).

A.6.3   Free energies and phase diagrams

Phase diagrams can display a large variety of features. As already mentioned, in materials physics the principal external parameters are temperature and composition. Therefore, for binary systems the phase space is two-dimensional, and therefore can be completely defined by a drawing.

A main point to remember is that a phase diagram is a reduction of the information contained in the free energy curves. Therefore, theoretically possible phase diagrams are exactly those for which continuously varying (in T and c) free energy curves can be found. Here the possible behaviours of free energy curves and the resulting features in the binary phase diagrams will be covered at hand of prototypical examples.

The first scenario is the miscibility gap (Fig. A.3). It appears in systems where interactions between unlike atoms are energetically costly. Therefore, the internal energy has a maximum at intermediate concentrations. The entropy on the other hand, qualitatively described by an expression such as (A.5.7), is convex, and will win at high temperatures over the internal energy to give a convex free energy. However, at some specific critical temperature the free energy will become non-convex. The corresponding single bitangent will therefore give a two-phase region that widens as temperature is further reduced. However, at any finite temperature there will be a finite solubility in each of the terminal phases, as the diverging derivative of the entropy at $c = 0$ and $c = 1$ always wins over the finite derivative of the internal energy.

The next cases correspond to the solid-liquid transition. If neither in the solid nor in the liquid phase there are large interactions but the melting temperatures of the pure elements deviate enough from each other, a situation as in Fig. A.4 results. The liquid has higher entropy as well as higher internal energy than the solid. Therefore, at low temperatures the solid has lower free energy. With rising temperature the difference becomes smaller, until at the melting temperature of the lower-melting element the two curves touch. At higher temperatures the bitangent points move towards the higher-melting concentration, and after the
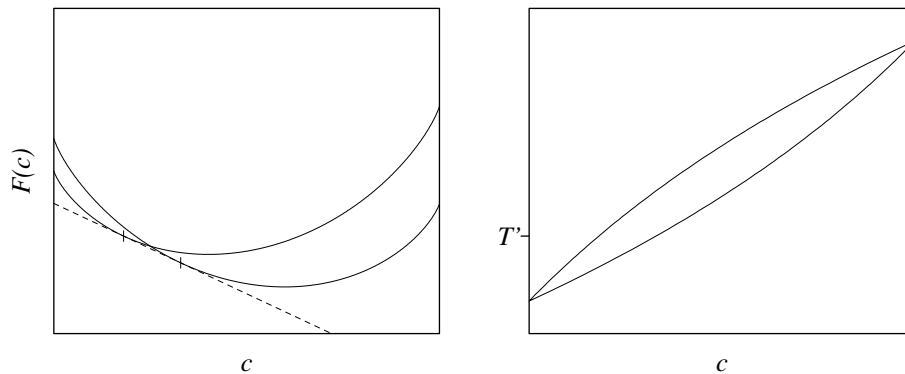
Figure A.4: Liquid-solid transition in ideally mixing case.
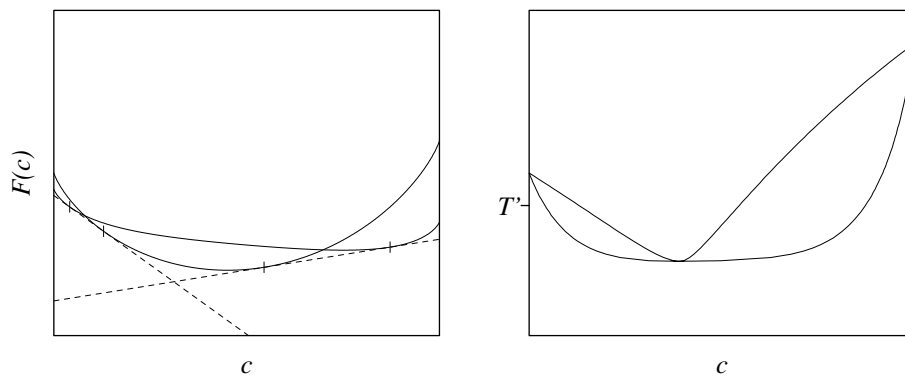

Figure A.5: Liquid-solid transition with demixing tendency in solid phase.

temperature has passed the melting temperature of the higher-melting element, the liquid has lower free energy over the whole concentration range. In this scenario, the *liquidus* line (over which the system is exclusively liquid) and the *solidus* line (below which it is solid) form a lense-shaped two-phase region of liquid and solid. Note that this shows that when cooling a system of some fixed composition the equilibrium concentration of solid and liquid phase vary with decreasing temperature. If the cooling happens fast so that the diffusion kinetics in the solid cannot follow, the resulting solid will show gradual concentration variations. This phenomenon is known as *Seigerung*.

If now there is a demixing tendency in the solid, the thermodynamical stability of the liquid will be higher at intermediate compositions. In this case, a situation as depicted in Fig. A.5 will result, where the liquidus line shows a minimum, corresponding to the point where the free energy curve of the liquid passes first through the solid's curve. At this point congruent solidification or melting is possible (i.e., at the same concentration and without long-range mass transport).

A system hosting a high-melting intermetallic phase leads to a situation as illustrated in Fig. A.6. Here the free energy curve of the intermetallic phase passes through the liquid free energy curve, again leading to a specific point of
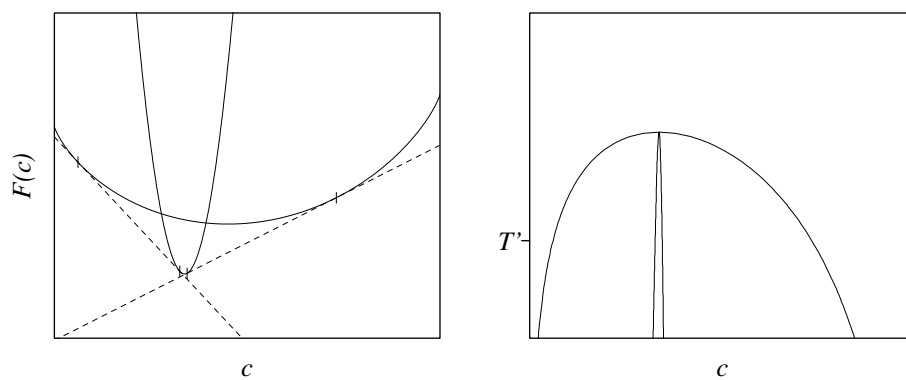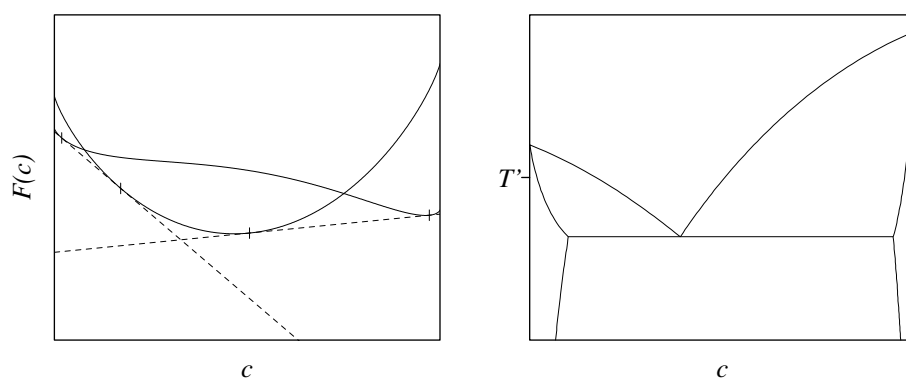
Figure A.6: High-melting intermetallic line phase.
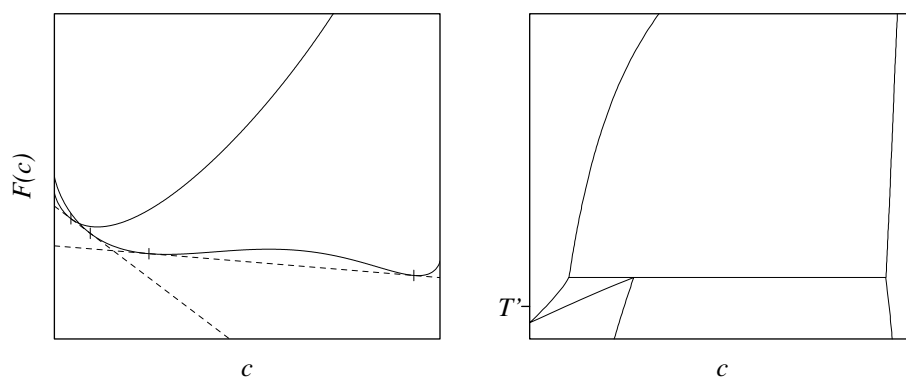

Figure A.7: Eutectic transition.

Figure A.8: Peritectic transition.

	above	below	type
homotectic	L	L' + L''	
monotectic	L	L' + S	eutectic
eutectic	L	$S_1 + S_2$	
catatectic	S_1	$S_2 + L$	
monotectoid	S_1	$S_1' + S_2$	eutectoid
eutectoid	S_1	$S_2 + S_3$	
syntectic	L + L'	S	peritectic
peritectic	$L + S_1$	S_2	
peritectoid	$S_1 + S_2$	S_3	peritectoid

Table A.4: Classification of invariant reactions in binary systems. Note that the homotectic and syntectic cases, corresponding to liquid phase separation, are normally not encountered in atomic as opposed to molecular systems.

congruent melting, where both bitangents disappear at the same time.

The final scenarios to treat correspond to the splitting of one bitangents into two, or equivalently the case where a single phase splits discontinuously into two phases when varying the temperature. If the single phase exists above the transition temperature, such transitions are said to be of *eutectic* or *eutectoid* type, for reactions involving at least one liquid phase or only solid phases, respectively. The cases of a single phase existing below the transition corresponds to reactions of *peritectic/peritectoid* type. These cases are illustrated in Figs. A.7 and A.8. The nomenclature for the possible cases (essentially pertaining to which participating phases are liquid and which are solid) is given in Tab. A.4. Specifically the eutectic transition gives a characteristic microstructure, with a fine succession of the solid product phases due to the limited diffusivity in the solid.

As an example, the Ni-Al binary system shall be discussed. Its phase diagram is given in Fig. A.9. It is dominated by the B2-NiAl intermetallic phase, which is congruently melting at practically stoichiometric composition due to its large thermodynamic stability. Its phase field is quite asymmetric due to the qualitatively different constitutional defects on the respective sides of stoichiometry as discussed in Sect. A.3.5. Indeed, the phase Al_3Ni_2 with $D5_{13}$ structure as discussed in Sect. A.2.3.1 can be understood as an ordering of the consitutional vacancies on the Ni-lean side of NiAl. It ends in a peritectic transition, which is shifted away from the ideal stoichiometry due to the stability of NiAl. The Al_3Ni phase is yet less stable and thus also ends in a peritectic transition. It is a line compound, that is, it has a very small capacity to incorporate an excess of either element, which is due to its complicated structure of type $D0_{11}$ (shared by cementite Fe_3C). Also in pure fcc Al, the solubility of Ni is extremely low (at most 0.11 at.%), thus the addition of Ni lowers the free energy of the liquid phase compared to the solid candidates, giving a eutectic point at about 3 at.% Ni.

On the other side, the solubility of Al in Ni is quite large, which leads to the solidus and liquidus lines extrapolating nicely to the melting temperature of Al. Further, the $L1_2$ Ni_3Al phase is just the superstructure due to an ordering of the dissolved Al atoms. Here there is a peculiar situation, as the eutectic temperature (as the low-temperature endpoint of the liquid phase in this region)
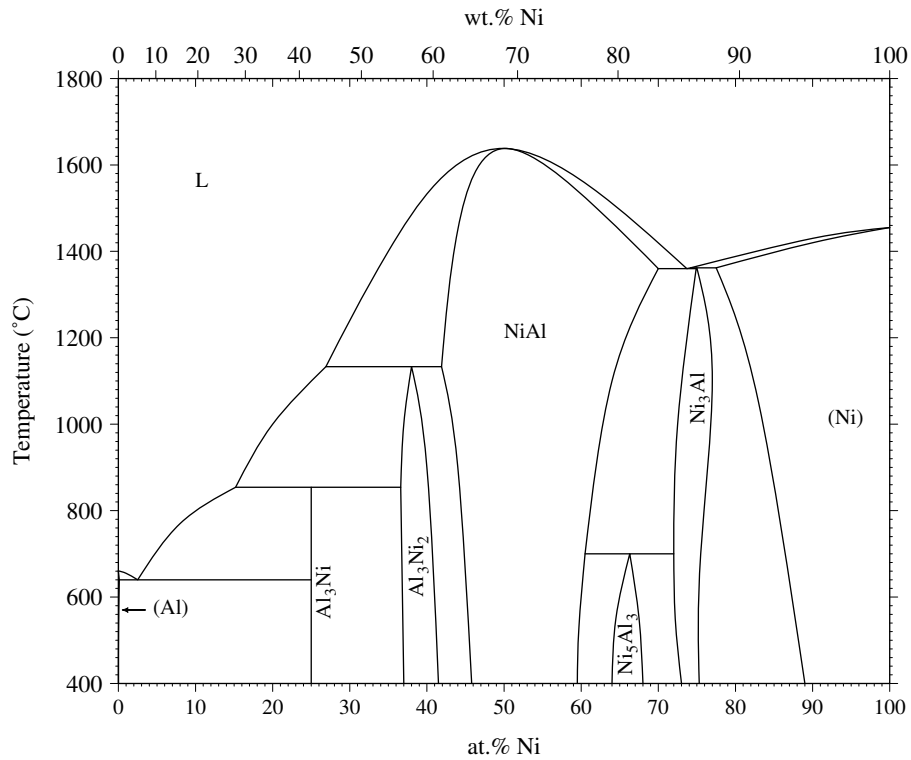
Figure A.9: Binary phase diagram of Ni-Al.

and the high-temperature endpoint of the Ni$_3$Al phase nearly coincide, making the experimental determination of the correct topology quite complicated. Nowadays it is assumed that the eutectic point is to the left of the Ni$_3$Al phase, which thus dissolves peritectically into the liquid phase and fcc Ni (as opposed to NiAl). The complicated Ni$_5$Al$_3$ is much less stable and ends in a peritectoid transition to NiAl and Ni$_3$Al.

For systems composed of more than two components, two-dimensional illustrations cannot capture the whole phase space. In the ternary case, conventionally one encodes the composition as the position within an equilateral triangle, where the corners correspond to the pure elements. Concentration-dependent quantities such as the liquidus temperature can then be specified, e.g., by drawing contour lines. Another possibility is to draw cuts through phase space at some specified temperature as illustrated in Fig. A.10 for the Ni-Mn-Al system. For compositions with not too high Al content, the system displays the terminal Ni (fcc) and Mn (A13) phases. Note that the A13 phase of Mn can accomodate about 35 at.% Al, while alloying Ni transforms it to an fcc phase (γ-Mn). Also the converse case of alloying Mn to Ni leads to an fcc structure over a wide range of compositions, while with Al the intermediate L1$_2$-phase is formed around the nominal composition of Ni$_3$Al as already obvious from the binary Ni-Al phase diagram. Finally, there is the B2 phase, which is characterized by Ni and Al splitting into different sublattices (corresponding to the prototypical B2 NiAl system in the binary limit)
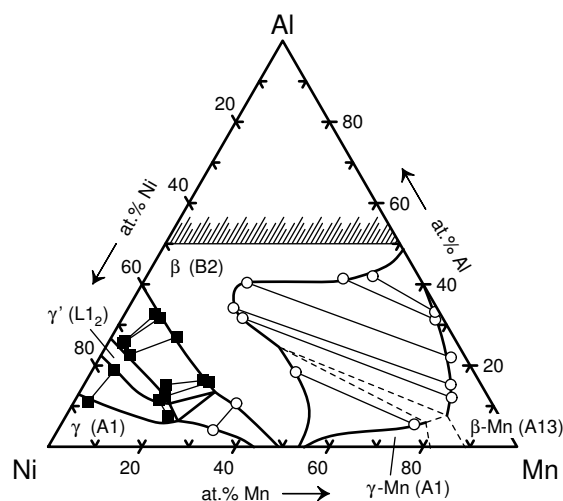
Figure A.10: Ternary phase diagram of Ni-Mn-Al at 850 °C (redrawn from R. Kainuma et al., *J. Alloys Comp.* **269**, 173 (1998)).

with Mn filling in on the sublattice of the deficient element. In the two-phase regions *tie lines* connect the bitangent points, i.e. for a given point in a two-phase region the system will decompose into two phases with respective compositions corresponding to the endpoints of the tie line the overall composition lies on, and weights as given by the lever rule. Note also the three-phase regions of strict triangular form at compositions of about $Ni_{65}Mn_{25}Al_{10}$ (where Ni-rich fcc, $L1_2$ and B2 are in equilibrium) and $Ni_{20}Mn_{65}Al_{15}$ (where β-Mn, Mn-rich fcc and B2 are in equilibrium). For any total composition within those regions, the system decomposes into three phases with compositions corresponding to the triangle corners and weights given by a generalized lever rule.

Gibbs' phase rule rationalizes the number of phases that can be in equilibrium: For constant pressure, it reads

$$f = n - P + 1, \tag{A.6.6}$$

where n is the number of components in the system, P is the number of phases in equilibrium, and f is the number of degrees of freedom (which encompass composition and temperature). For instance, if in a three-component system ($n = 3$) there are three phases in equilibrium ($P = 3$), there is only one degree of freedom left, which is the temperature, as all concentrations are fixed. As another example, in a two-component system the region of a homogeneous phase has two degrees of freedom (temperature and composition), while in a two-phase region the compositions directly follow from the temperature.

Finally, as an example for a pressure-temperature phase diagram the case of iron is illustrated in Fig. A.11. Already at zero pressure iron is a peculiar case: At low temperatures it has a ferromagnetic bcc structure, the only ferromagnetic phase. Within this α phase there is a Curie transition to a paramagnetic bcc structure, soon followed by a transition to fcc. However, before the system eventually melts, it transforms back to bcc. As can be expected, higher pressures favour close-packed
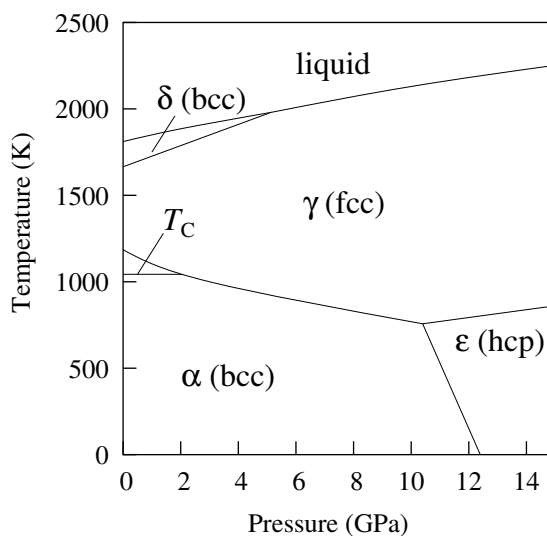
Figure A.11: The pressure-temperature phase diagram of iron.

phases, where additional to the widening fcc phase an hcp phase appears at low temperatures. Indeed, the hcp phase is the most stable phase under pressure, as the fcc phase ends at a critical point at about 80 GPa and 2800 K, after which hcp is the sole stable solid phase.

Qualitatively, the widening of the γ-phase region with temperature implies that the fcc phase is favoured by compression over the bcc phases. Specifically, consider the α and γ-phases. As γ is the high-temperature phase, it has a higher specific internal energy. The negative slope of the phase boundary implies that compressing the system favours the γ phase, therefore this phase has to have a higher density. Quantitatively, this is captured by the Clausius-Clapeyron relation

$$\frac{\mathrm{d}P(T)}{\mathrm{d}T} = \frac{L}{T \Delta v},$$

(A.6.7)

where $P(T)$ is the phase boundary, L the specific latent heat and Δv the specific volume change during the transition. Note that this relation is meaningful only for first-order transitions, having non-zero latent heat and volume change.

As a consequence of the above, one can directly infer the sign of the volume change at a phase transition from pT-phase diagrams: A negative slope of the phase boundary implies an increase of the density when going from the low-temperature to the high-temperature phase and vice versa. For the case of iron this corresponds to $\rho_L < \rho_\delta < \rho_\gamma < \rho_\epsilon$, $\rho_\alpha < \rho_\gamma$ as well as $\rho_\alpha < \rho_\epsilon$.